FRICTION PENDULUM DOUBLE CONCAVE BEARING

Technical Report

Prepared by

Professor Michael C. Constantinou
University at Buffalo
State University of New York, Buffalo, NY

October 29, 2004

1. INTRODUCTION

This report provides technical documentation for the Friction Pendulum-Double Concave (FP-DC) seismic isolation bearing. The FP-DC bearing is an adaptation of the traditional, well-proven single concave FP bearing that allows for significantly larger displacements for identical FP bearing plan dimensions. This document and its revisions can be used to support the use of FP-DC bearings on building, bridge and infrastructure projects in the United States and abroad

The next five sections of this report present the following information on FP-DC bearings:

- Principles of operation.
- Derivation of force-displacement relations, decomposition of motion on sliding surfaces, sensitivity on property variability and calculation of effective properties.
- Experimental results.
- List of applications of FP-DC bearings
- Analysis and design considerations for FP-DC bearings.

An earthquake-simulator testing program is soon to be undertaken at the University at Buffalo that will involve four model-scale FP bearings. The results of those tests will be reported in another report. The author of this report will be the lead investigator for this earthquake-simulator project.

This report contains seven sections and two appendices. Figures follow the references, which appear in Section 7. Appendices A and B, which present force-displacement loops from large-scale FP-DC bearing tests, follow the figures.

2. FP-DC BEARING PRINCIPLES OF OPERATION

This section of the report describes the principles of operation of the FP-DC bearing. Figure 1 shows sections through a FP-DC bearing at the three stages of lateral displacement: 1) zero displacement; 2) displaced with sliding on the lower concave surface only; and 3) maximum displacement. A discussion of the response of the FP-DC bearing at each of these stages is presented below.

Zero displacement

The bearing consists of two facing concave surfaces. The upper and lower concave surfaces have radii of curvature R_1 and R_2, respectively, that might not be equal. The coefficients of friction on these two sliding surfaces are m_1 and m_2, respectively. An articulated slider separates the two concave surfaces. The articulation is necessary for proper distribution of pressure on the sliding surfaces and to accommodate differential movements along the top and bottom sliding surfaces. Figures 2 to 4 show views of a small-scale FP-DC bearing tested at the University at Buffalo in October 2004. The bearing components are shown in Figures 2 and 3 where the articulated slider is shown assembled and disassembled in the two figures. The assembled bearing is shown in Figure 4.

Displaced with sliding on the lower concave surface only

In Figure 1b, the bearing is shown to undergo sliding on the lower concave surface only. This is possible when the coefficient of friction on the lower sliding interface is less than the coefficient of friction on the upper sliding surface, that is, $m_2 < m_1$. In Section 3 of this report, it is shown that initially sliding occurs on the surface with the least friction and is followed by sliding on both surfaces regardless of either the radii of curvature or the values of coefficient of friction of the two interfaces. In these cases, sliding will be at unequal displacement increments on the two surfaces.

Maximum displacement

The displacement capacity of the bearing equals $2d$, where d is the maximum displacement on a single concave surface. This dimension is shown in Figure 1.

Section 3 provides more information on the operation of the FP-DC bearing and proves that

1. The condition of sliding on one concave surface occurs only at initial movement and generally will involve only small lateral displacements.

2. When sliding commences simultaneously on both concave surfaces, the restoring (spring) force F_r is given by

$$F_r = \frac{W}{R_1 + R_2 - h_1 - h_2} \cdot u \qquad (1)$$

   where u is the displacement of the upper concave plate with respect to the lower concave plate (i.e., the bearing displacement) and W is the vertical compressive load on the bearing. The friction force F_f is given by

$$F_f = \frac{m_1 (R_1 - h_1) W + m_2 (R_2 - h_2) W}{R_1 + R_2 - h_1 - h_2} \tag{2}$$

3. Most applications of FP-DC bearings will likely utilize concave surfaces of equal radii, namely, $R_1 = R_2$. Part heights of the articulated slider, h_1 and h_2 are nearly equal in most cases. If $R_1 = R_2$ and $h_1 = h_2$, the bearing behaves as a standard FP bearing with effective coefficient of friction equal to the average of m_1 and m_2.

3. FORCE-DISPLACEMENT RELATIONS OF FP-DC BEARING

In deriving the force-displacement relation of the FP-DC bearing, motion on the top sliding surface and then on the bottom sliding surface is considered separately. Consider the configuration shown in Figure 1(a) and assume that the slider is fixed to the bottom concave plate that displaces to the right under the action of a lateral force. As a result, the slider moves on the top concave plate. Figure 5 shows a free body diagram of the articulated slider. The forces acting on the slider are:

1. The vertical load, W, which acts at the pivot point.

2. The lateral force, F_1, transferred through the bottom part of the bearing and acting on the top part of the slider.

3. The friction force, F_{f1}, acting on the sliding interface.

4. The normal force, S_1, acting on the sliding interface (shown off-center of the slider so that moment equilibrium is satisfied).

5. Friction traction along the spherical surface of the articulated slider.

Equilibrium of the slider in the vertical and horizontal directions gives:

$$W - S_1 \cos\theta_1 + F_{f1} \sin\theta_1 = 0 \tag{3}$$

$$F_1 - S_1 \sin\theta_1 - F_{f1} \cos\theta_1 = 0 \tag{4}$$

By geometry,

$$u_1 = (R_1 - h_1)\sin\theta_1 \tag{5}$$

where u_1 is the movement of the slider on the top concave surface. Combining equations (3), (4) and (5), gives

$$F_1 = \frac{W}{(R_1 - h_1)\cos\theta_1} u_1 + \frac{F_{f1}}{\cos\theta_1} \tag{6}$$

A similar analysis of equilibrium for sliding on the bottom concave surface gives:

$$u_2 = (R_2 - h_2)\sin\theta_2 \tag{7}$$

and

$$F_2 = \frac{W}{(R_2 - h_2)\cos\theta_2} u_2 + \frac{F_{f2}}{\cos\theta_2} \tag{8}$$

where u_2 is the movement of the slider on the bottom concave surface, F_2 is the lateral force transferred through the top part of the bearing and acting on the bottom part of the slider, F_{f2} is the friction force acting on the bottom sliding surface of the slider and q_2 is the angle of rotation of the bottom part of the articulated slider.

Equations (3) to (8) can be simplified when angles q_1 and q_2 are small so that $\cos q_1 \approx \cos q_2 \approx 1$, $\sin q_1 \approx q_1$ and $\sin q_2 \approx q_2$ to give

$$F_1 = \frac{W}{R_1 - h_1} u_1 + F_{f1} \tag{9}$$

$$F_2 = \frac{W}{R_2 - h_2} u_2 + F_{f2} \tag{10}$$

The total movement (displacement) of the bearing is

$$u = u_1 + u_2 \tag{11}$$

Furthermore, the horizontal component of the force transferred through the bearing (excluding the insignificant inertia forces associated with the moving parts of the bearing) is:

$$F = F_1 = F_2 \tag{12}$$

Using equations (9) through (12):

$$F = \left(\frac{W}{R_1 + R_2 - h_1 - h_2} \right) u + \left(\frac{F_{f1}(R_1 - h_1) + F_{f2}(R_2 - h_2)}{R_1 + R_2 - h_1 - h_2} \right) \tag{13}$$

$$u_1 = \left(\frac{F - F_{f1}}{W} \right) (R_1 - h_1) \tag{14}$$

$$u_2 = \left(\frac{F - F_{f2}}{W} \right) (R_2 - h_2) \tag{15}$$

Equation (13) is valid when sliding occurs on both concave surfaces. It is valid for displacement u larger than a limit u^*, which is established as follows.

Let $F_{f1} = m_1 W$, $F_{f2} = m_2 W$ and assume that $m_1 < m_2$. Upon the application of a lateral force F on the bearing, sliding will occur on the top concave surface where the coefficient of friction is smallest. Motion will continue with $u = u_1$, $u_2 = 0$, and $F = F_1$ where F_1 is given by (9). This condition will continue until $F = F_1 = F_{f2}$. Thereafter, sliding will occur on both surfaces and (13) is valid. Equating F_1 in (9) to F_{f2} gives:

$$u^* = (m_2 - m_1)(R_1 - h_1) \tag{16}$$

A sample force-displacement relationship for a FP-DC bearing is shown in Figure 6. Consider the following two combinations of geometry and friction.

Combination 1

The two concave surfaces have equal radii, so that $R_1 - h_1 = R_2 - h_2 = 84\text{in.} = 2134\text{mm}$. Let the nominal friction coefficient be 0.05 but due to variability in the properties $m_1 = 0.045$ and $m_2 = 0.055$. This situation might be typical of FP-DC bearings. It follows that $u^* = 0.84\text{in.} = 21.3\text{mm}$ and the effective coefficient of friction, m_e, given by the second term in (13) upon division by W is 0.05:

$$m_e = \frac{m_1(R_1 - h_1) + m_2(R_2 - h_2)}{R_1 + R_2 - h_1 - h_2} \tag{17}$$

The resulting force-displacement relationship is shown in Figure 7(a).

Combination 2

In combination 2, the FP-DC bearing has $R_1 - h_1 = 39\text{in.} = 991\text{mm}$, $R_2 - h_2 = 120\text{in.} = 3048\text{mm}$, $m_1 = 0.03$, and $m_2 = 0.06$: a bearing with a significant restoring force and re-centering capability for weak seismic excitation. In this case, $u^* = 1.17\text{in.} = 29.7\text{mm}$ and $m_e = 0.0526$. The resulting force-displacement relationship is shown in Figure 7(b).

For the typical FP-DC bearing of Figure 7(a), namely, $R_1 - h_1 = R_2 - h_2$ and $m_1 \approx m_2$, the bearing behavior can be represented by a rigid-linear model with characteristic strength equal to $m_e W$ and stiffness equal to $W/(R_1 + R_2 - h_1 - h_2)$. The bearing behavior of Figure 7(b) warrants representation using a rigid-bilinear model.

4. EXPERIMENTAL RESULTS

Section 4 of the report presents three sets of data from tests of FP-DC bearings with concave surfaces of equal radii.

Dataset 1

Dataset 1 involves tests of a small-scale FP-DC bearing at the University at Buffalo. The test bearing is shown in Figures 2 to 4. A drawing of the bearing is shown in Figure 8. (Note that the ring retainer of the bearing was machined to remove material in order to be able to instrument the bearing and to observe the interior movement during testing-compare Figure 8 to Figure 4). The bearing consists of two identical concave plates of 18.65 in. radius of curvature and a slider of 3 in. in diameter and 2.65 in. height. It has a displacement capacity of ±6 in. Figures 9 to 11 present views of the bearing in the testing machine at the University at Buffalo at various stages of deformation. The cable of the transducer (string pot) used to measure the displacement of the slider on the top concave surface is visible in these figures. Moreover, the relative displacement of the top and bottom concave surfaces was directly measured, allowing for decomposition of the motion to the two components on the two concave surfaces.

Results of two tests are reported herein. Both were conducted under the following conditions: vertical load of 13.3 kip, 3 fully-reversed cycles of sinusoidal lateral motion at amplitude of 4.0 in. and frequency of 0.1 Hz. The peak velocity in the tests was 2.5 in/sec (64 mm/sec), however the peak sliding velocity was less but generally exceeding 1.0 in/sec (2.5 in/sec is the velocity of the top concave surface with respect to the bottom concave surface-it is not the peak sliding velocity). The material used at the sliding interface typically exhibits peak friction at sliding velocities exceeding 1.0 in/sec (this is the material identified as PTFE composite No.1 in Constantinou et al, 1999).

The two tests were conducted under different frictional conditions at the sliding interfaces:

1. With the two sliding interfaces having nearly identical frictional properties. For this case, Figure 12 presents the recorded histories of bearing displacement and velocity, and Figure 13 presents the recorded normalized lateral force-lateral displacement loops. The velocity histories were obtained by numerical differentiation of the displacement records. The normalization of the lateral force is by the normal force in order to easily extract the frictional characteristics. In this case, $R_1 - h_1 = 18.65 - 1.40 = 17.25 in. = 438 mm$ and $R_2 - h_2 = 18.65 - 1.25 = 17.4 in. = 442\ mm$ (top surface is denoted as surface 1) and the friction coefficients on the two sliding surfaces are nearly identical. The result is rigid-linear behavior as depicted in Figure 12 and identical sliding motions on the two concave surfaces as demonstrated in the displacement and velocity histories in Figure 13. The effective friction coefficient is $m_e = 0.05$. This implies that $m_1 \approx m_2 = 0.05$. Observations of the bearing during testing (video is available) confirmed that sliding on the two concave surfaces was concurrent.

2. With the bottom sliding interface lubricated so that the two sliding interfaces have substantially different frictional properties. The recorded histories of bearing displacement and velocity are presented in Figure 14 and the recorded loops are presented in Figure 15. Observations during testing (video is available) confirmed that sliding initiated on the bottom surface (surface of least friction), that on reversal of motion sliding initially occurred only on the bottom surface and that the histories of motion on the two surfaces were different. The rigid-bilinear nature of the recorded loops is consistent with the theory presented in Section 3. Specifically, the effective coefficient of friction was obtained from the recorded normalized force at zero displacement

as $m_e = 0.0359$. The coefficient of friction on the lubricated bottom sliding interface was determined as one half of the drop in the normalized force on reversal of motion to be $m_2 = 0.0168$ (to derive this value, a reconstruction of the loop at maximum displacement was needed given the "rounding" of the loops due to velocity effects on the value of the friction). The coefficient of friction on the top sliding surface was then calculated by use of (17) to be $m_1 = 0.055$. This value is consistent with what was obtained in the testing of the un-lubricated bearing ($m_1 \approx m_2 = 0.05$, so that it could be that $m_1 = 0.055$). The two slopes of the ascending branch of the recorded normalized loops were determined by graphical means to be 1/17.0 in.$^{-1}$ and 1/35.4 in.$^{-1}$. The theoretical expressions for the normalized stiffness are $1/(R_1 - h_1)$ and $1/(R_1 + R_2 - h_1 - h_2)$, respectively, giving values of 1/17.4 in.$^{-1}$ and 1/34.7 in.$^{-1}$. Thus, the measured values of stiffness are within 2% of the theoretically derived values. Moreover, the value of sliding displacement on the bottom concave surface during reversal of motion after reaching maximum displacement is $2u^*$, where $u^* = (m_1 - m_2)(R_2 - h_2)$ as given by (16) but with subscripts 1 and 2 interchanged (the bottom surface is of lower friction rather than the top one). The measured value of $2u^*$ is 1.35 in. and the theoretical value is $2u^* = 2(m_1 - m_2)(R_2 - h_2) = 2(0.055 - 0.0168)17.4 = 1.33\text{in}$, which is in very good agreement with the measured value. Figure 16 illustrates the reconstruction of the loop and the graphical estimation of parameters.

Dataset 2

Figure 17 shows the geometric characteristics of the bearing. Figure 18 presents views of the bearing during testing in the large bearing testing machine of Earthquake Protection Systems, Inc., Vallejo, California. The bearing consists of two identical concave plates with a radius of curvature of 61 in. (1549 mm). The effective radius is $R_1 - h_1 + R_2 - h_2 = 113.5\text{in.} = 2883\text{mm}$. The bearing was tested at the slow speed (1 in./sec = 25 mm/sec) the machine is currently capable of achieving. The experimental force-displacement loops presented in Appendix A were recorded in tests at normal temperature with 1 to 4 cycles of imposed motion at amplitude of up to 8 in. (203 mm), peak velocity of 1 in/sec (25 mm/sec) and vertical load in the range of 250 to 1,270 kip (1,113 to 5,652 kN). The average bearing pressure on the slider is in the range of 2, 630 to 13,370 psi (18.1 to 92.2 MPa). The data in Appendix A show the following:

1. The behavior of the FP-DC bearing is rigid-elastic: the expected behavior of a FP-DC bearing with concave surfaces of equal radii and nearly equal friction coefficients for each of the two sliding surfaces. Under such conditions, sliding occurs simultaneously and by equal amounts on the two concave surfaces.

2. The effective radius of curvature, $R_1 - h_1 + R_2 - h_2$, can be verified from the second slope of the hysteresis loop. The theory predicts correctly the slope of the loop.

3. The effective coefficient of sliding friction for the bearing is in the range of about 0.04 to 0.05, depending on the bearing pressure.

Dataset 3

This dataset was collected from tests of FP-DC bearings installed in the Teslin Bridge in Yukon, Canada: a bridge rehabilitated in 2004 using FP-DC bearings. Appendix B presents drawings of the two types of bearings used in this bridge. The bearings include concave parts with equal radii of curvature and nearly identical coefficients of sliding friction. The test results presented in Appendix B are force-displacement loops for the *large type* bearing at three different vertical loads, normal temperature and speeds less than or equal to 25 mm/sec. The tested bearing has $R_1 = R_2 = 39\,\text{in.} = 991\text{mm}$ and an effective radius of curvature of 74 in. (1880 mm). The force-displacement loops exhibit rigid-linear behavior with a stiffness consistent with an effective radius of curvature of 74 in.

5. APPLICATIONS OF FP-DC BEARINGS

FP-DC bearings were first applied in Japan on a small number of buildings. Information exists only for one of these buildings since it was instrumented and experienced a small earthquake on June 7, 2000. The building is the Technical Research Laboratory of Magara Construction Company in Ishikawa (Hyakuda et al., 2001). The building has a total floor area of 15,770 square feet (=1,465 square meters), is two-stories in height, is constructed of reinforced and prestressed concrete and is supported by 12 FP-DC bearings with each concave surface having a radius equal to 98.4 in. (2,500 mm). The bearings are subjected to an average pressure of about 2,500 psi (17.5 MPa) and have an effective coefficient of sliding friction at large sliding velocities (above 200 mm/sec) equal to about 0.04. The earthquake of June 7, 2000 produced peak ground acceleration at the site of 0.149 g, which although low, was sufficient to activate the FP-DC bearings. Table 5.1 below presents peak values of recorded acceleration response in the two principal horizontal directions of the building.

Table 5.1: Recorded Response of the Managa Construction Research Laboratory

Location	*Peak acceleration EW direction (g)*	*Peak acceleration NS direction (g)*
Roof	0.069	0.125
First floor	0.054	0.089
Base above isolators	0.068	0.096
Ground below isolators	0.079	0.149

A displacement recorder in the building provided information on the peak isolation system displacement, equal to 5mm. There was no permanent displacement. Analysis showed a peak displacement of 6 mm, which is consistent with the observed 5 mm, and a permanent displacement of about 2 mm. The beneficial effects of isolation were clearly evident in this building even though the bearing displacements were very small. See Tsopelas et al. (1996a, 1996b) for experimental results that support this behavior for sliding isolation systems.

The first application of FP-DC bearings in North America is the Teslin Bridge, Yukon, Canada. This bridge was rehabilitated in 2004 using the two types of FP-DC bearings of Appendix B. Eight bearings of the *large type* and 28 bearings of the *small type* were used.

6. ANALYSIS AND DESIGN CONSIDERATIONS FOR FP-DC BEARINGS

This section contains information on (a) *P-D* moment transfer by FP-DC bearings, (b) modeling of FP-DC bearings for dynamic analysis, and (c) property modification factor analysis and suggested values of λ-factors for FP-DC bearings.

$\mathrm{P}-\Delta$ Moment Transfer by FP-DC Bearings

Herein P is defined is the axial load on the bearing and Δ is defined as the bearing displacement (relative displacement of the top concave plate with respect to the bottom concave plate). While in conventional FP bearings the $\mathrm{P}-\Delta$ moment is transferred on the side of the (single) concave plate, in the FP-DC bearing the $\mathrm{P}-\Delta$ moment is divided among the two concave plates. The moments transferred to the top and bottom concave plates are given by $P \times u_1$ and $P \times u_2$, respectively, where u_1 and u_2 are given by equations (14) and (15). In the case of FP-DC bearings with $R_1 - h_1 = R_2 - h_2$ and $m_1 \approx m_2$, displacements u_1 and u_2 are each effectively equal to $\frac{\Delta}{2}$ and the moment transferred on each concave plate is equal to $\frac{\mathrm{P} \cdot \Delta}{2}$.

Modeling of FP-DC Bearings for Dynamic Analysis

Modeling of FP-DC bearings in commonly used computer programs for the dynamic analysis is of seismically isolated structures (e.g., SAP2000 and 3D-BASIS) is currently possible only in the case in which $R_1 - h_1 = R_2 - h_2$ and $m_1 \approx m_2$. This situation might be typical of FP-DC bearings. The behavior of the bearing can be modeled as that of a conventional FP bearing with radius of curvature equal to $R_1 - h_1 + R_2 - h_2$ and coefficient of friction as determined by experiment. The velocity dependence of the coefficient of friction is typically described by

$$\mu = f_{max} - (f_{max} - f_{min}) exp(-a|V|) \tag{18}$$

where V is the velocity of the top concave plate with respect to the bottom concave plate, f_{max} and f_{min} are, respectively the sliding coefficients of friction at large velocity of sliding and at nearly zero velocity of sliding and a is parameter that controls the transition from f_{min} to f_{max}. Typically only parameter f_{max} is determined in the prototype bearing testing program, whereas parameter f_{min} is selected on the basis of available experimental results (e.g., as described in Constantinou et al, 1999). Parameter a is also selected on the basis of available experimental results. For example, Constantinou et al, 1999 suggest a value of 100 *sec/m* for interfaces consisting of polished stainless steel and the PTFE composite used in FP bearings for building applications. However, in FP-DC bearings the velocity of relevance is the one on the sliding interfaces which is less than velocity V. For FP-DC bearings with $R_1 - h_1 = R_2 - h_2$ and $m_1 \approx m_2$, the velocity on each sliding interface is nearly equal to $V/2$. Therefore, equation (18) may be used for FP-DC bearings but with parameter a having half value or 50 *sec/m* for the typical interface used in building applications.

Property Modification Factor Analysis and Suggested Values of l-Factors

The concept of bounding analysis on the basis of system property modification factors or λ-factors is described in Constantinou et al (1999) and it is found in the 1999 AASHTO Guide Specifications for Seismic Isolation Design. The method is a systematic procedure for calculating upper and lower bound values for the mechanical properties of seismic isolators given due account to aging, contamination, history of loading, temperature and other effects. For FP bearings, only the coefficient of friction is a parameter that is affected by the aforementioned effects. The system property modification factors for FP-DC bearings are the same as those of conventional (single concave) FP bearings except for the case of the contamination factor. That factor should be calculated as the weighted average of the contamination factor values for the two interfaces, of which the one is facing down (interface 1) and the other is facing up(interface 2):

$$\lambda_c = \frac{\lambda_{c1}\mu_1(R_1 - h_1) + \lambda_{c2}\mu_2(R_2 - h_2)}{\mu_1(R_1 - h_1) + \mu_2(R_2 - h_2)} \tag{19}$$

where λ_{c1} and λ_{c2} are the λ-factors for contamination of interfaces 1 and 2, respectively. In the case of FP-DC bearings with $R_1 - h_1 = R_2 - h_2$ and $m_1 \approx m_2$, λ_c becomes the average of λ_{c1} and λ_{c2}.

As an example consider FP-DC bearings with $R_1 - h_1 = R_2 - h_2$ and $m_1 \approx m_2$. The nominal value of the coefficient of friction is 0.05. The conditions of operation of the bearings are: (a) normal environment (non-corrosive), (b) bearings will be sealed in order to prevent contamination, (c) application is in a building structure so that cumulative travel is not considered, (d) bearings will be in controlled environment so that low temperature effects are not considered, (e) lifetime for the bearings is 30 to 50 years, (f) the sliding interfaces are not lubricated, and (g) the application is important so that adjustments on the λ-factors to account for the very small probability of concurrent occurrence of several extreme events (maximum earthquake, maximum corrosion, etc.) will not be considered.

A nominal value of 0.05 for the coefficient of friction implies that values of the coefficient of friction of fresh (non-aged) bearings under normal temperature conditions will be in the following ranges (these ranges will have to be specified in the project specifications):

1. For each tested bearing, the 3-cycle value (this is the average of three values, each determined in one of three consecutive cycles of testing)of the coefficient of friction at large velocity of sliding is in the range of 0.04 to 0.06.

2. Among all tested bearings, the average 3-cycle value of the coefficient of friction at large velocity of sliding is in the range of 0.045 to 0.055.

3. Among all tested bearings, the average value of the first cycle coefficient of friction at large velocity of sliding is less than 0.06.

Therefore, the minimum and maximum values of the coefficient of friction at large velocity of sliding (values of f_{max}) are 0.045 and 0.060, respectively.

The λ-factors are as follows (Constantinou et al, 1999 and AASHTO, 1999) For aging, $l_{a}=1.1$ (normal environment and sealed bearing); for contamination on the top sliding interface $l_{c1}=1.0$ (sealed, non-lubricated interface facing down); and for contamination on the bottom sliding interface $l_{c2}=1.1$ (sealed, non-lubricated interface facing up). On the basis of equation (19), $l_{c}=1.05$. Without adjustments, the value of the λ-factor is $l_{max}=l_{a}\cdot l_{c}=1.1\times 1.05=1.155$.

The upper and lower values of the coefficient of friction f_{max} for analysis are:

Lower bound value: 0.045

Upper bound value: $l_{max}\times 0.06=1.115\times 0.06=0.069$.

7. REFERENCES

American Association of State Highway and Transportation Officials – AASHTO (1999), "GUIDE SPECIFICATIONS FOR SEISMIC ISOLATION DESIGN", Washington, D.C.

Constantinou, M.C., Tsopelas, P., Kasalanati, A. and Wolff, E.D. (1999), "PROPERTY MODIFICATION FACTORS FOR SEISMIC ISOLATION BEARINGS", Report No. MCEER-99-0012, Multidisciplinary Center for Earthquake Engineering Research, Buffalo, NY.

Hyakuda, T. Saito, K., Matsushita, T., Tanaka, N., Yoneki, S., Yasuda, M., Miyazaki, M., Suzuki, A., and Sawada, T. (2001), "THE STRUCTURAL DESIGN AND EARTHQUAKE OBSERVATION OF A SEISMIC ISOLATION BUILDING USING FRICTION PENDULUM SYSTEM", Proceedings, 7th International Seminar on Seismic Isolation, Passive Energy Dissipation and Active Control of Vibration of Structures, Assisi, Italy, October 2-5.

Tsopelas, P., Constantinou, M.C., Kim, Y-S and Okamoto, S. (1996a), "EXPERIMENTAL STUDY OF FPS SYSTEM IN BRIDGE SEISMIC ISOLATION," <u>Earthquake Engineering and Structural Dynamics,</u> Vol. 25, No. 1, pp. 65-78.

Tsopelas, P., Constantinou, M.C., Okamoto, S., Fujii, S. and Ozaki, D. (1996b), "EXPERIMENTAL STUDY OF BRIDGE SEISMIC SLIDING ISOLATION SYSTEMS," <u>Engineering Structures,</u> Vol. 18, No. 4, pp. 301-310.

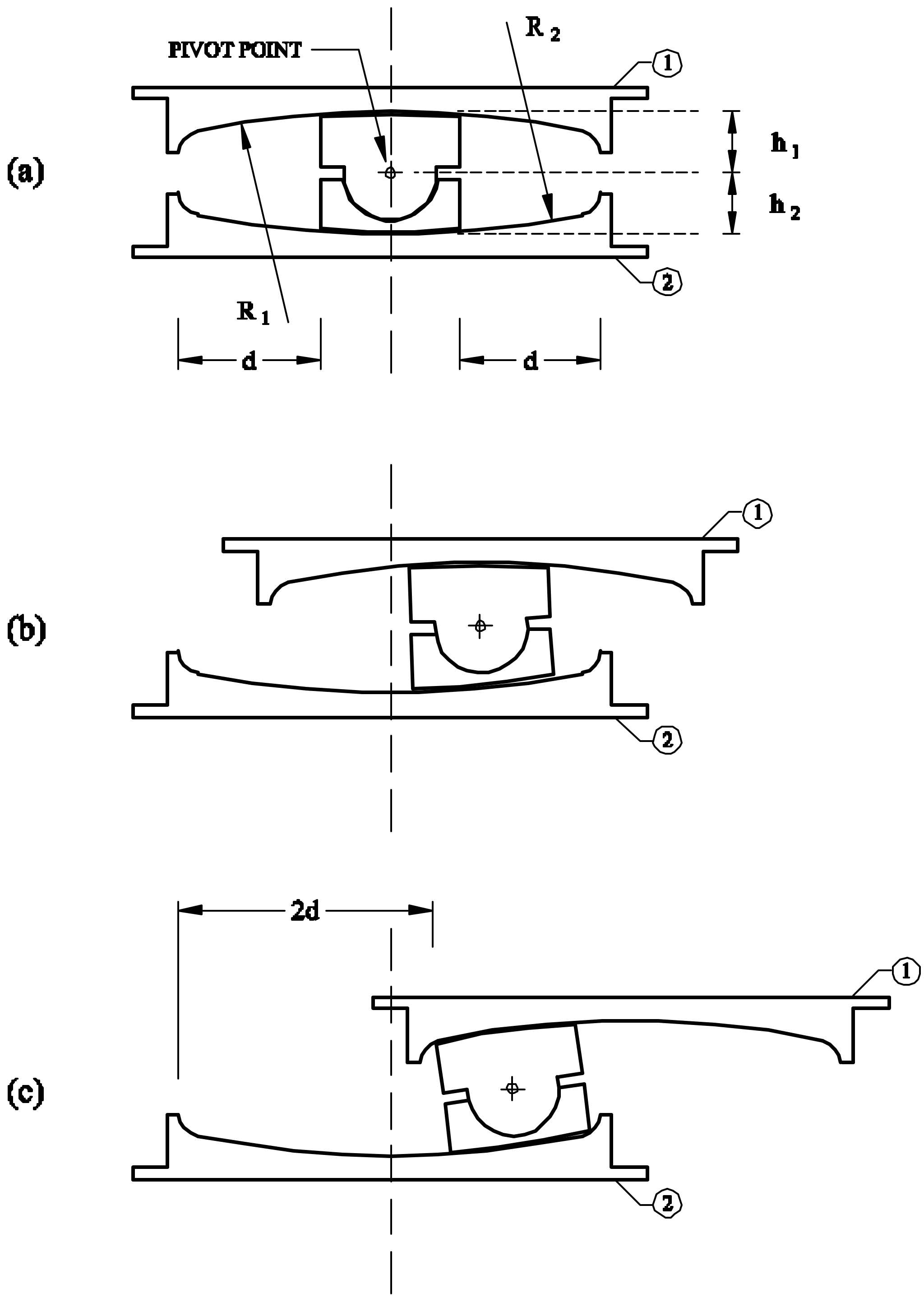

Figure 1: Section through a FP-DC Bearing, (a) zero displacement, (b) displaced with sliding on the lower concave surface only, and (c) maximum displacement

Figure 2: Small-scale FP-DC bearing with assembled articulated slider

Figure 3: Small-scale FP-DC bearing with disassembled articulated slider

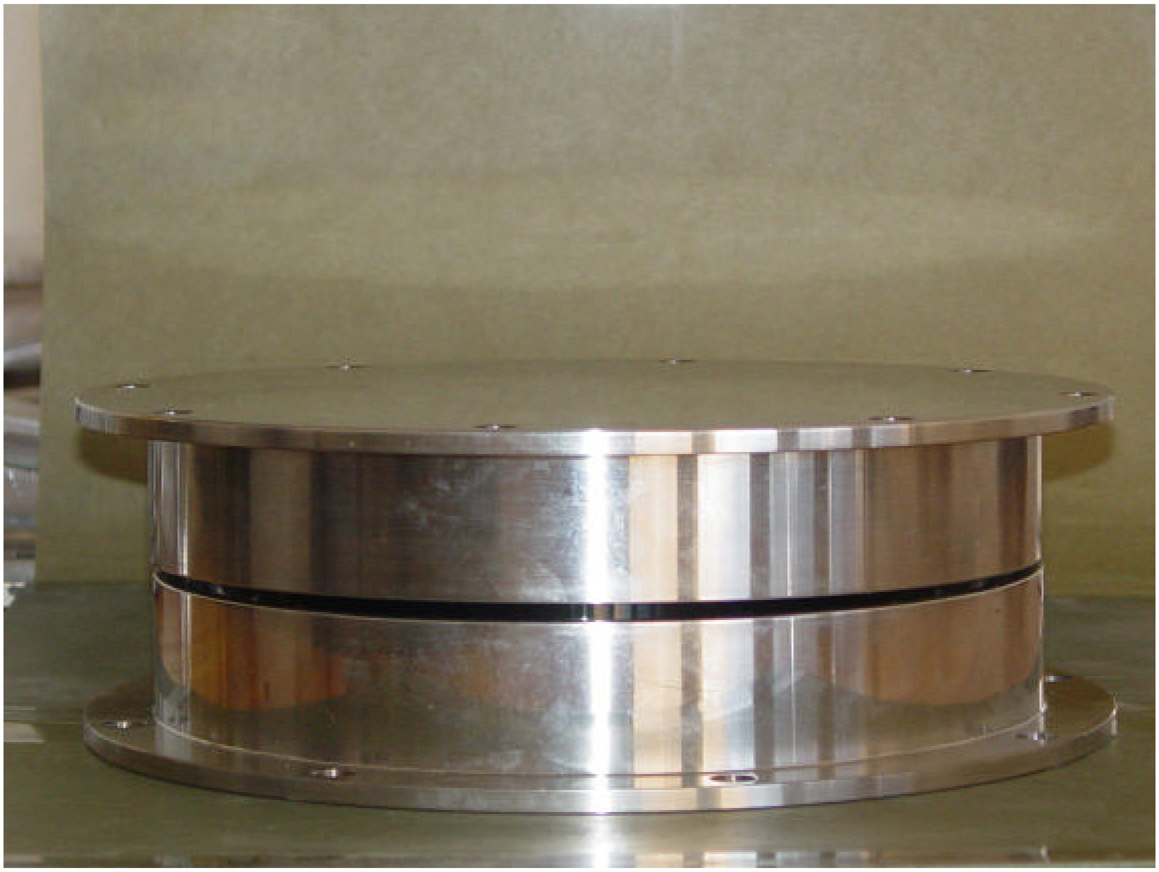

Figure 4: Assembled small-scale FP-DC bearing

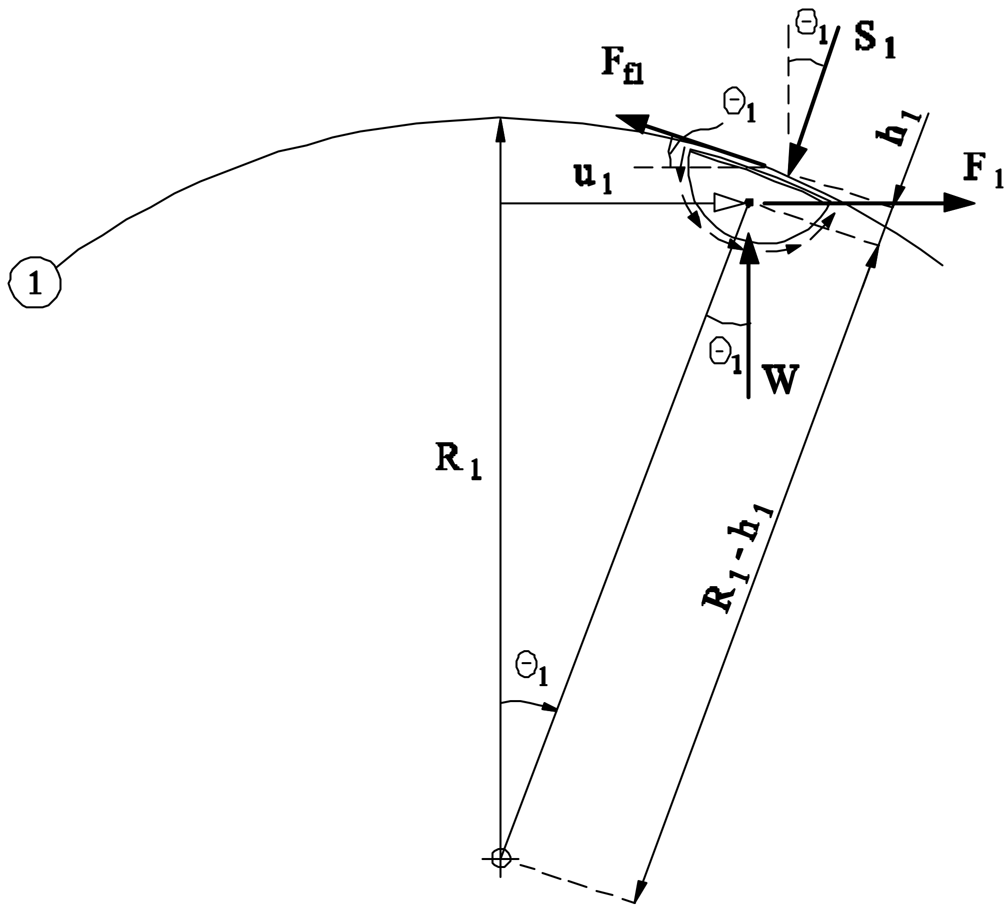

Figure 5: Free body diagram of articulated slider of FP-DC bearing during sliding on the upper concave surface

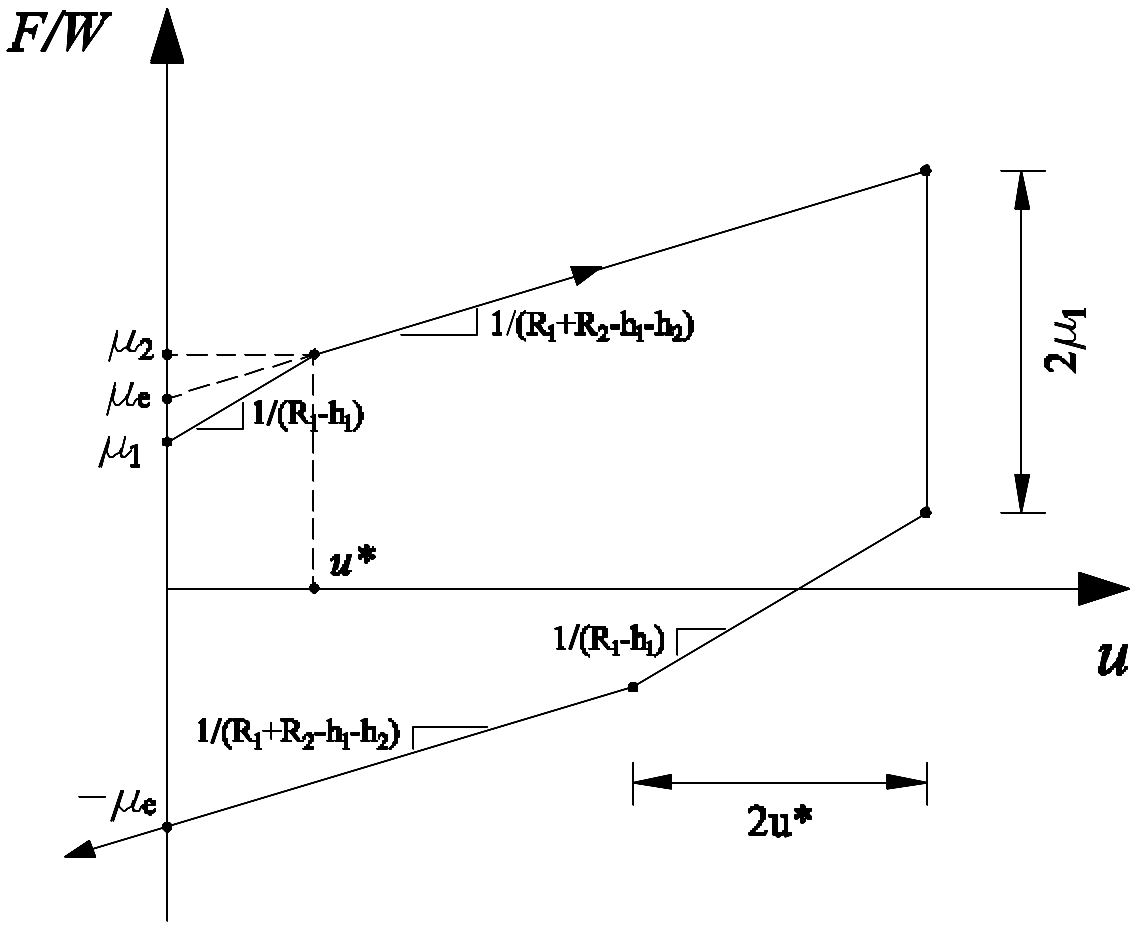

$$\mu_e = [\mu_1(R_1-h_1)+\mu_2(R_2-h_2)] \,/\, (R_1+R_2-h_1-h_2)$$

$$u^* = (\mu_2-\mu_1)(R_1-h_1)$$

Figure 6: Generic force-displacement relation of FP-DC bearing

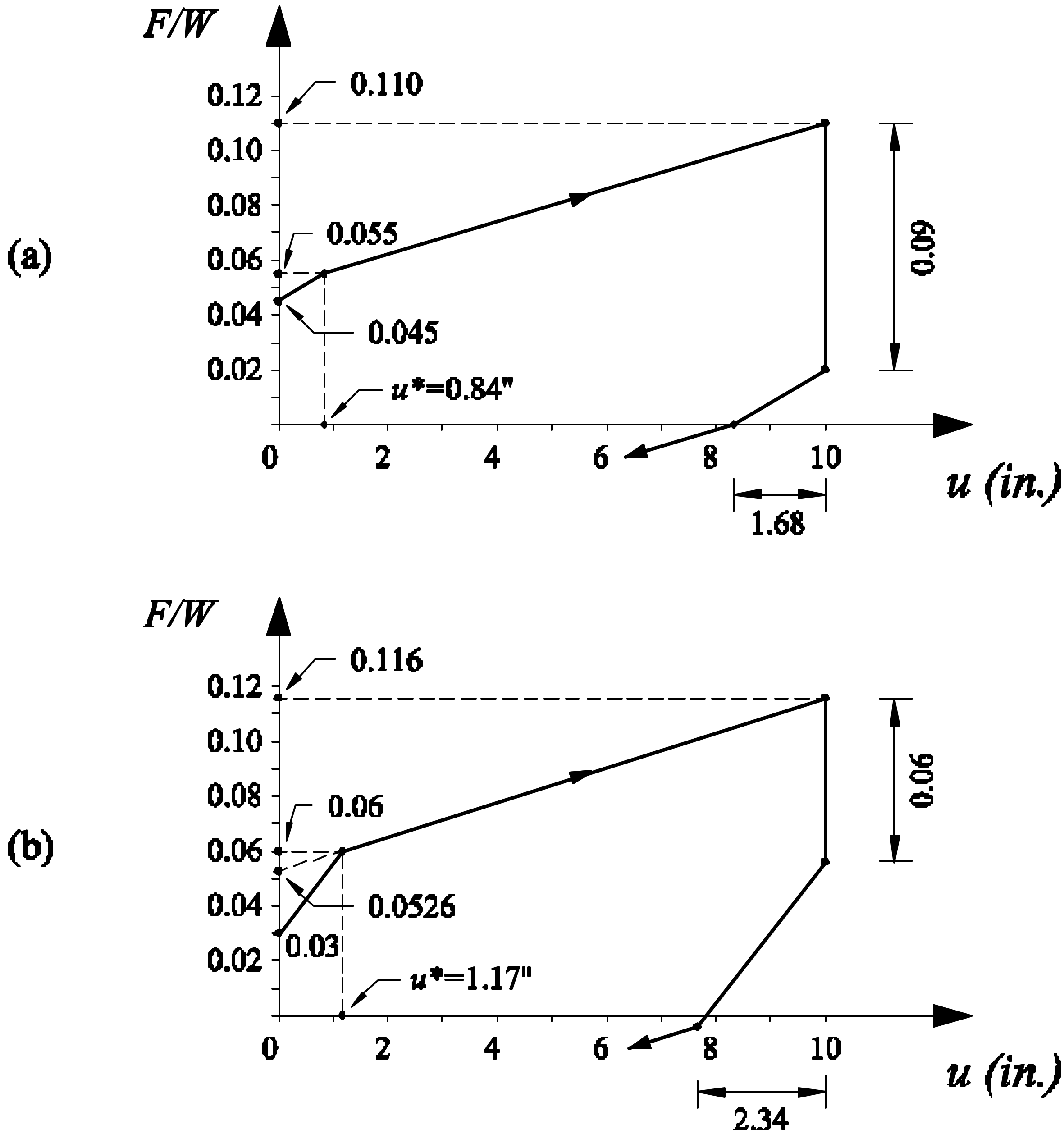

Figure 7: Force-displacement relationships for FP-DC bearings

(a) R_1-h_1=R_2-h_2=84 in., μ_1=0.045, μ_2=0.055

(b) R_1-h_1=39 in., R_2-h_2=120 in., μ_1=0.03, μ_2=0.06

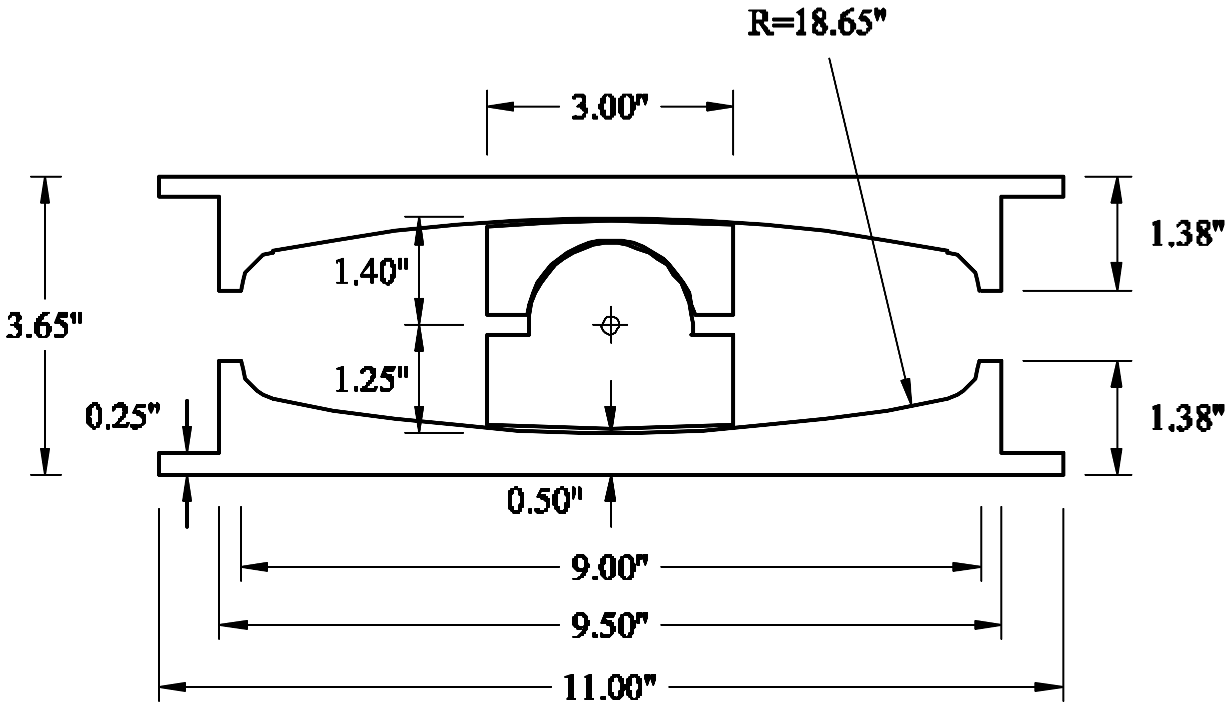

Figure 8: Small scale FP-DC bearing tested at the University at Buffalo

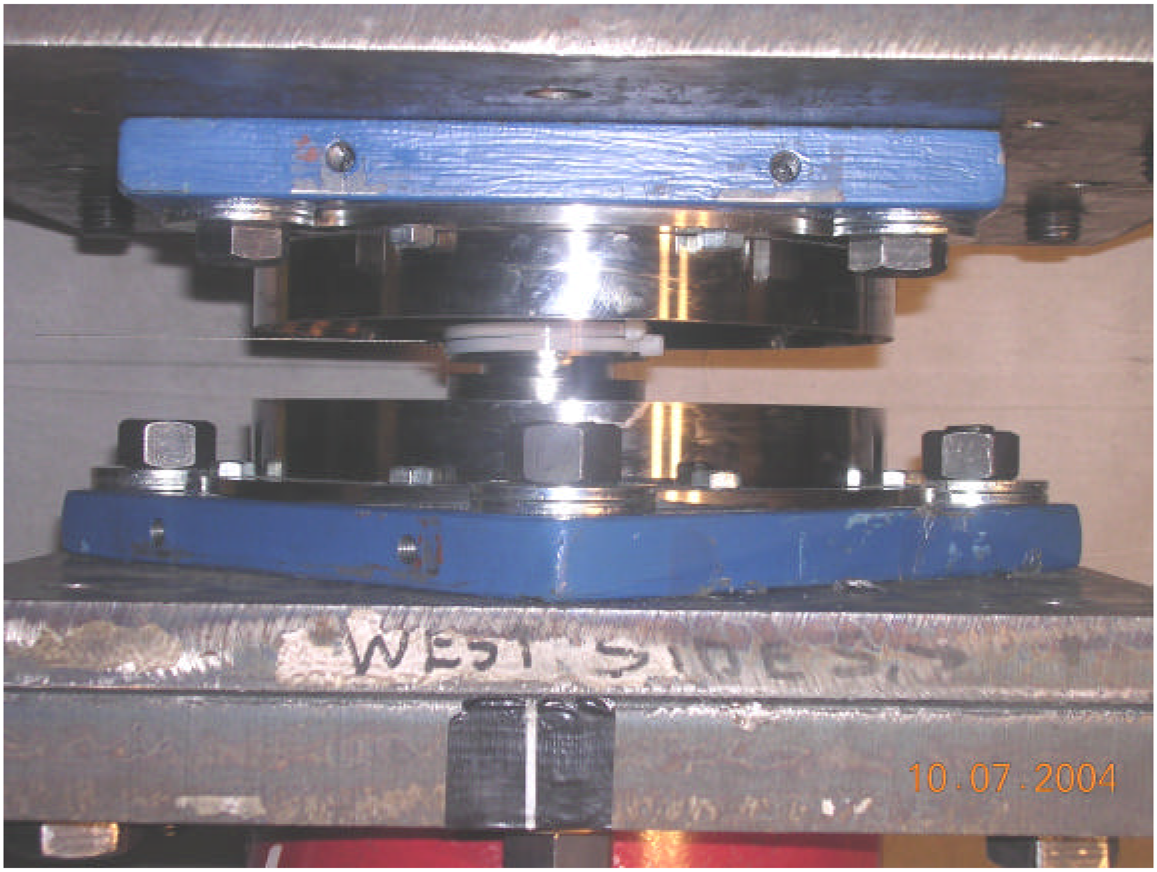

Figure 9: View of small scale FP bearing in testing machine at the University at Buffalo

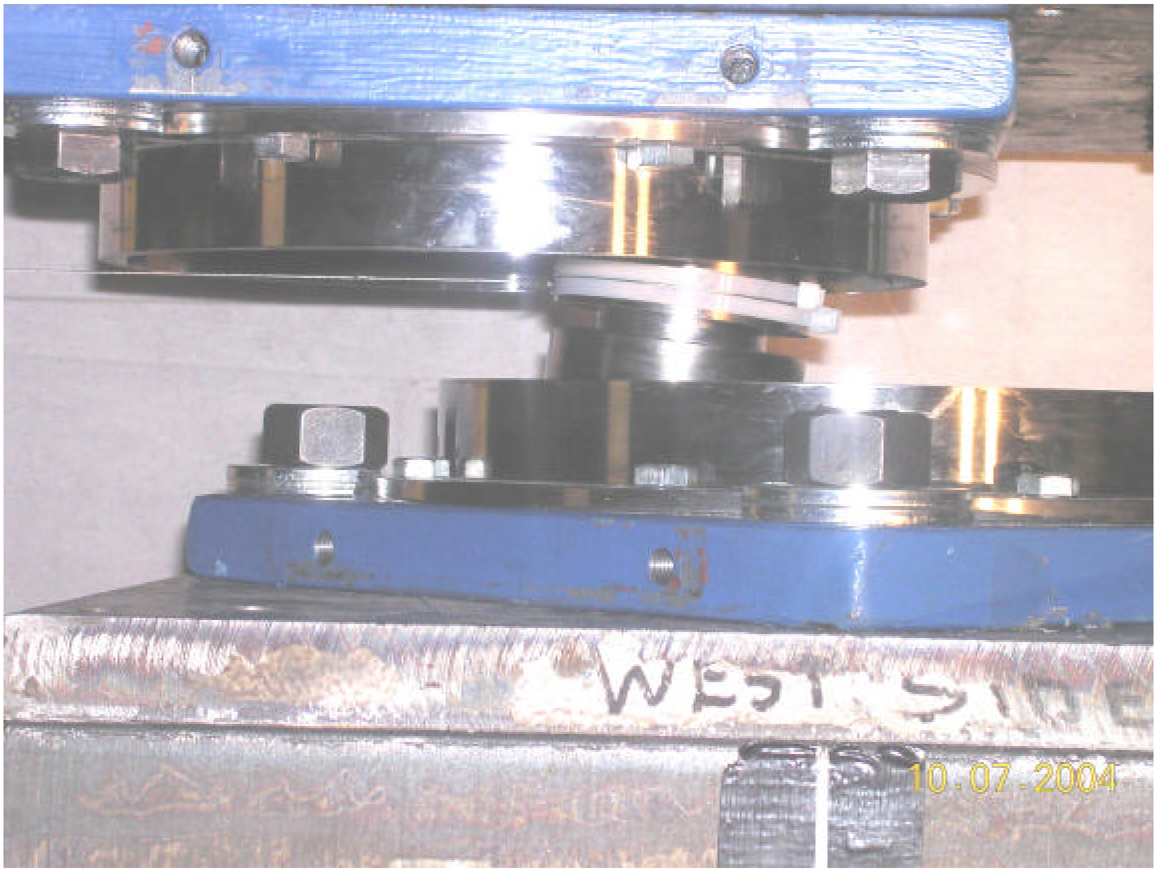

Figure 10: View of small scale FP bearing at extreme negative displacement during testing at the University at Buffalo

Figure 11: View of small scale FP bearing at extreme positive displacement during testing at the University at Buffalo

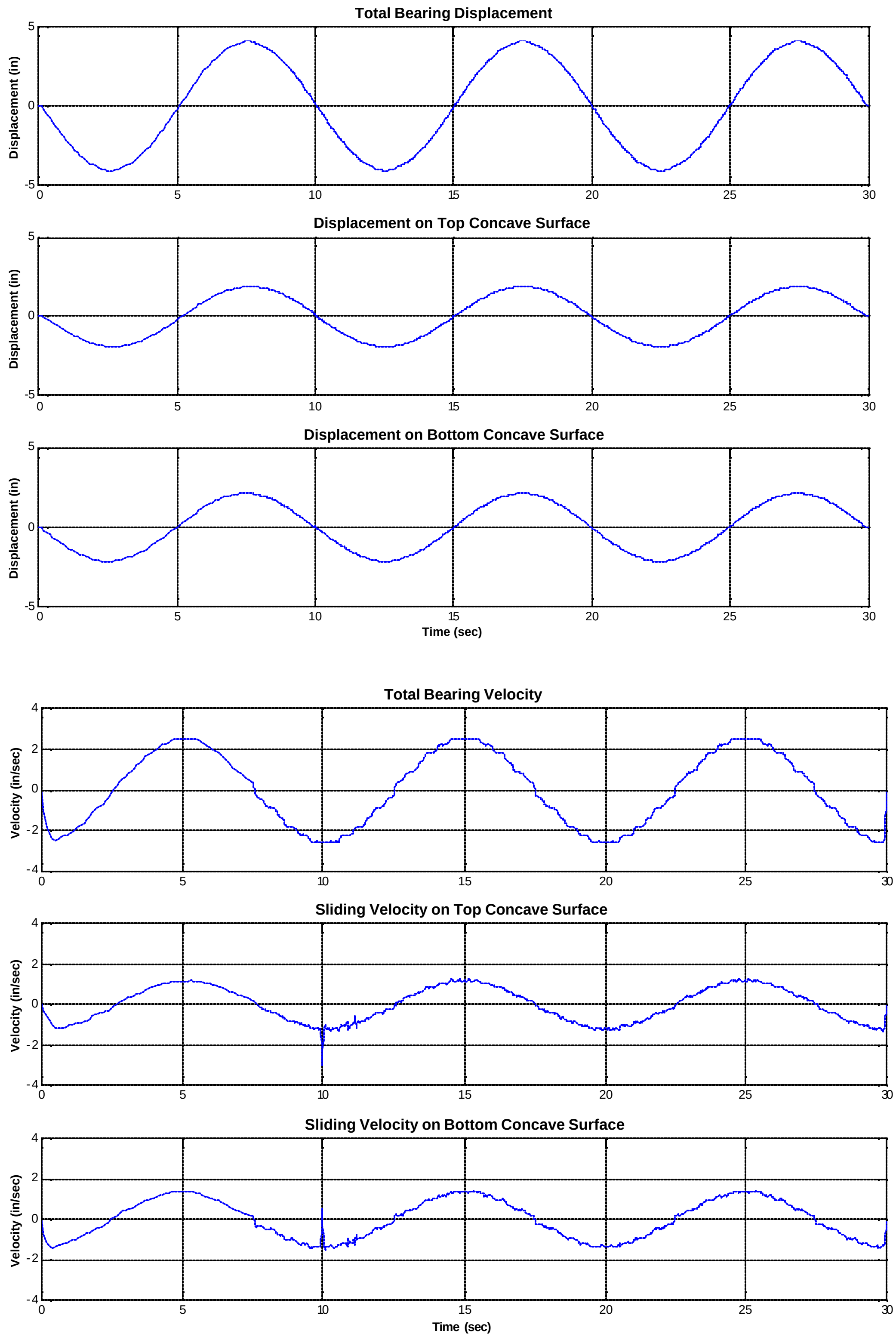

Figure 12: Recorded histories of displacement and velocity in test on small scale FP bearing with nearly equal coefficients of friction at the two sliding interfaces

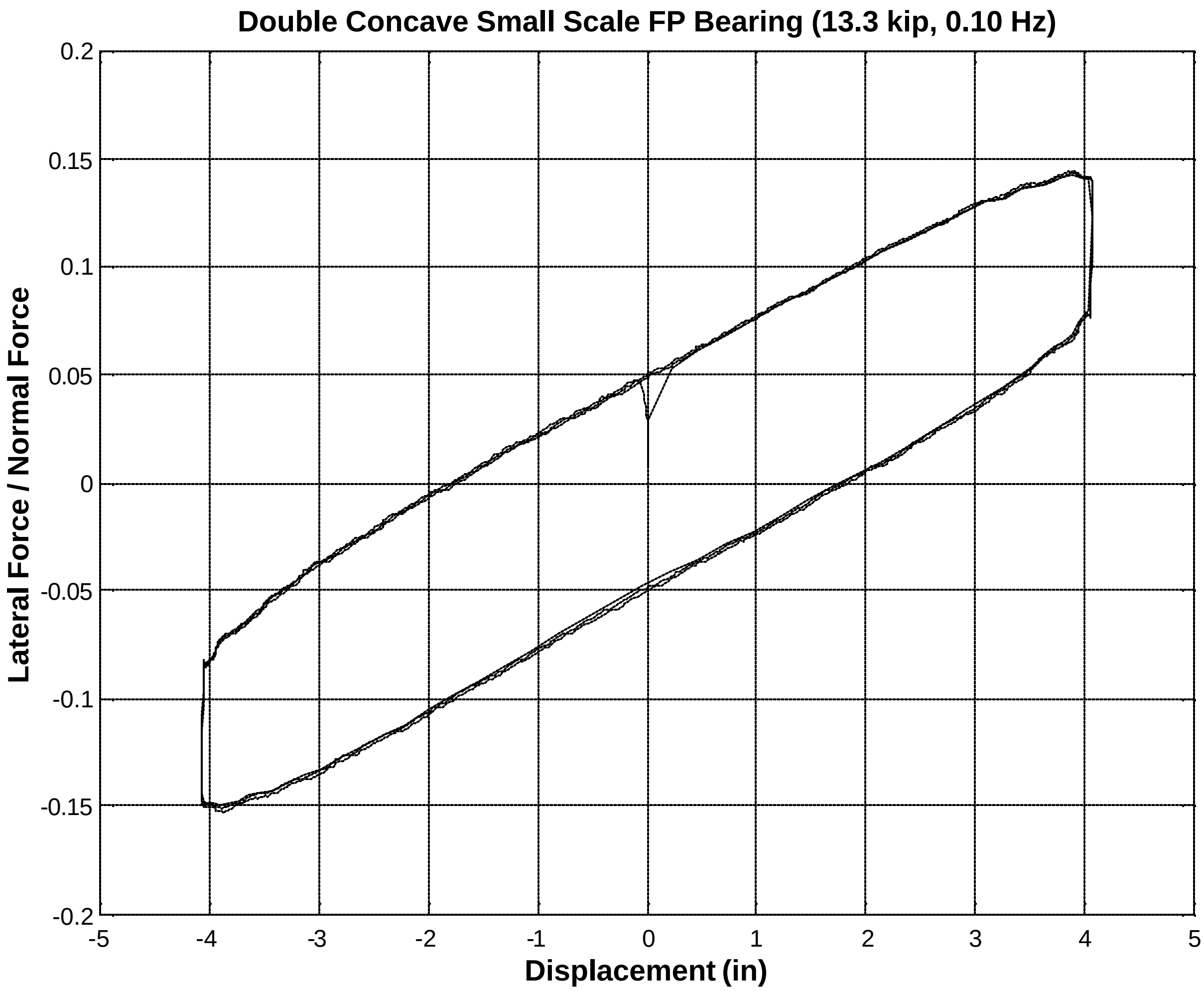

Figure 13: Recorded loops of normalized lateral force-lateral displacement in test on small scale FP bearing with nearly equal coefficients of friction at the two sliding interfaces

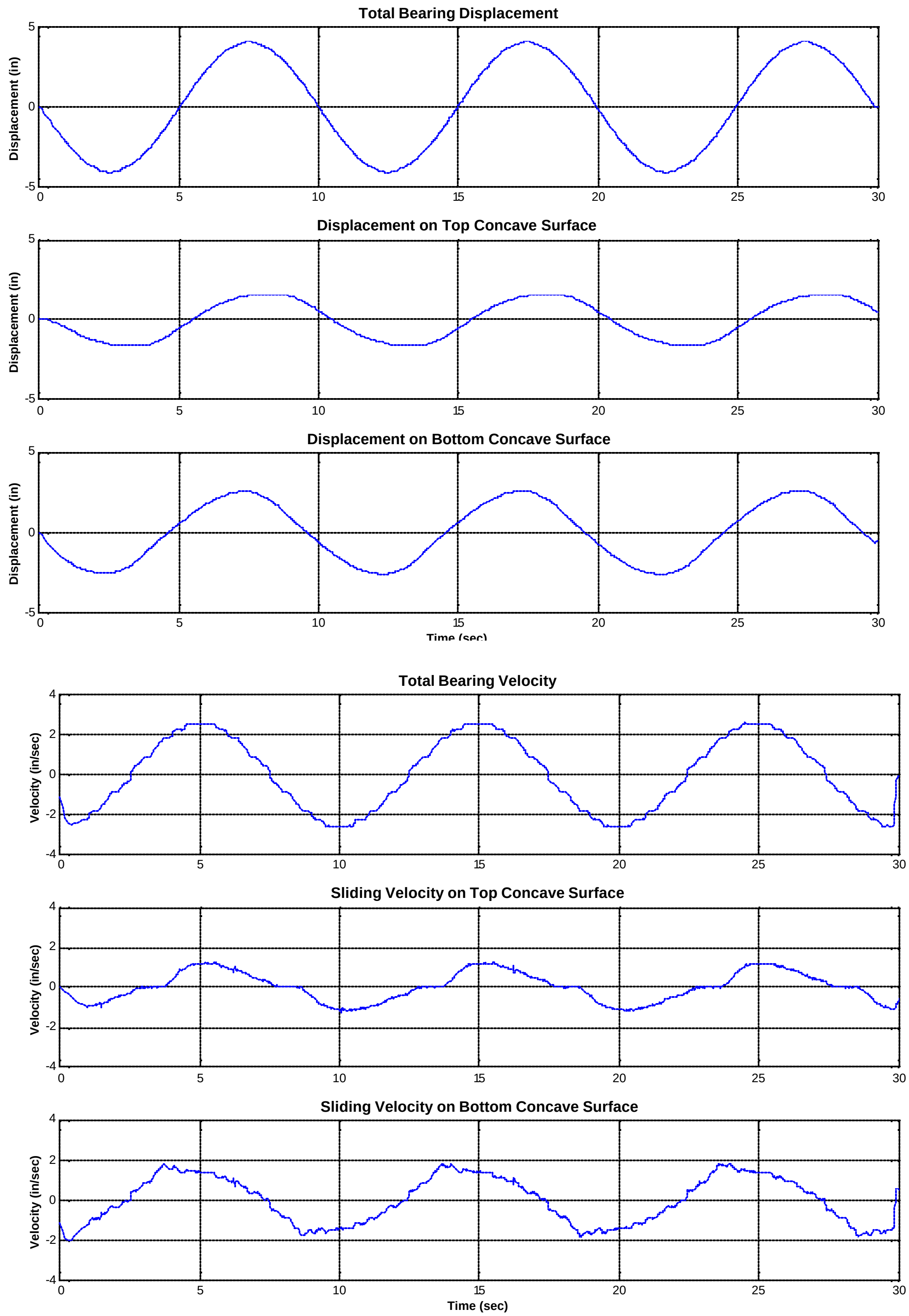

Figure 14: Recorded histories of displacement and velocity in test on small scale FP bearing with unequal coefficients of friction at the two sliding interfaces

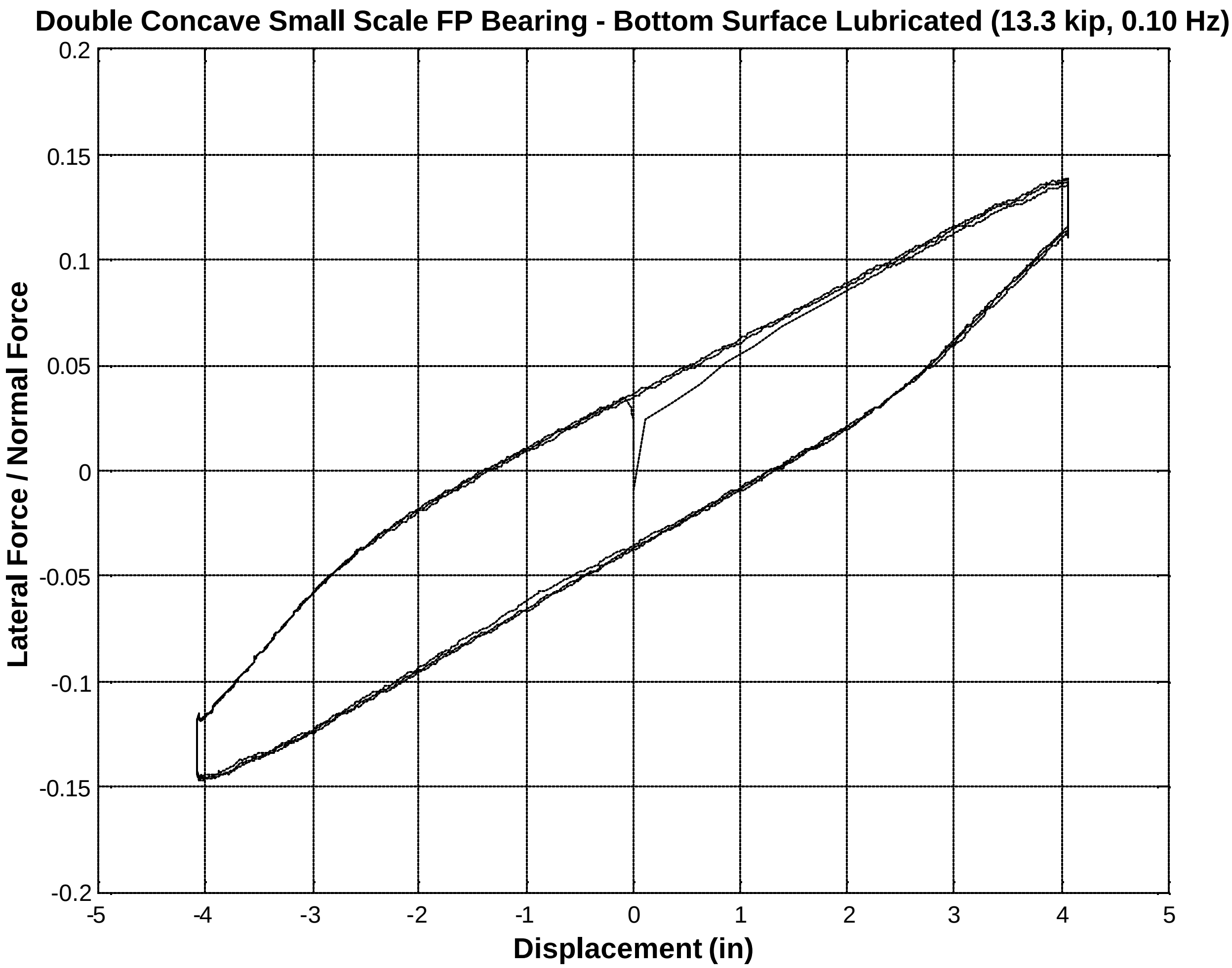

Figure 15: Recorded loops of normalized lateral force-lateral displacement in test on small scale FP bearing with unequal coefficients of friction at the two sliding interfaces

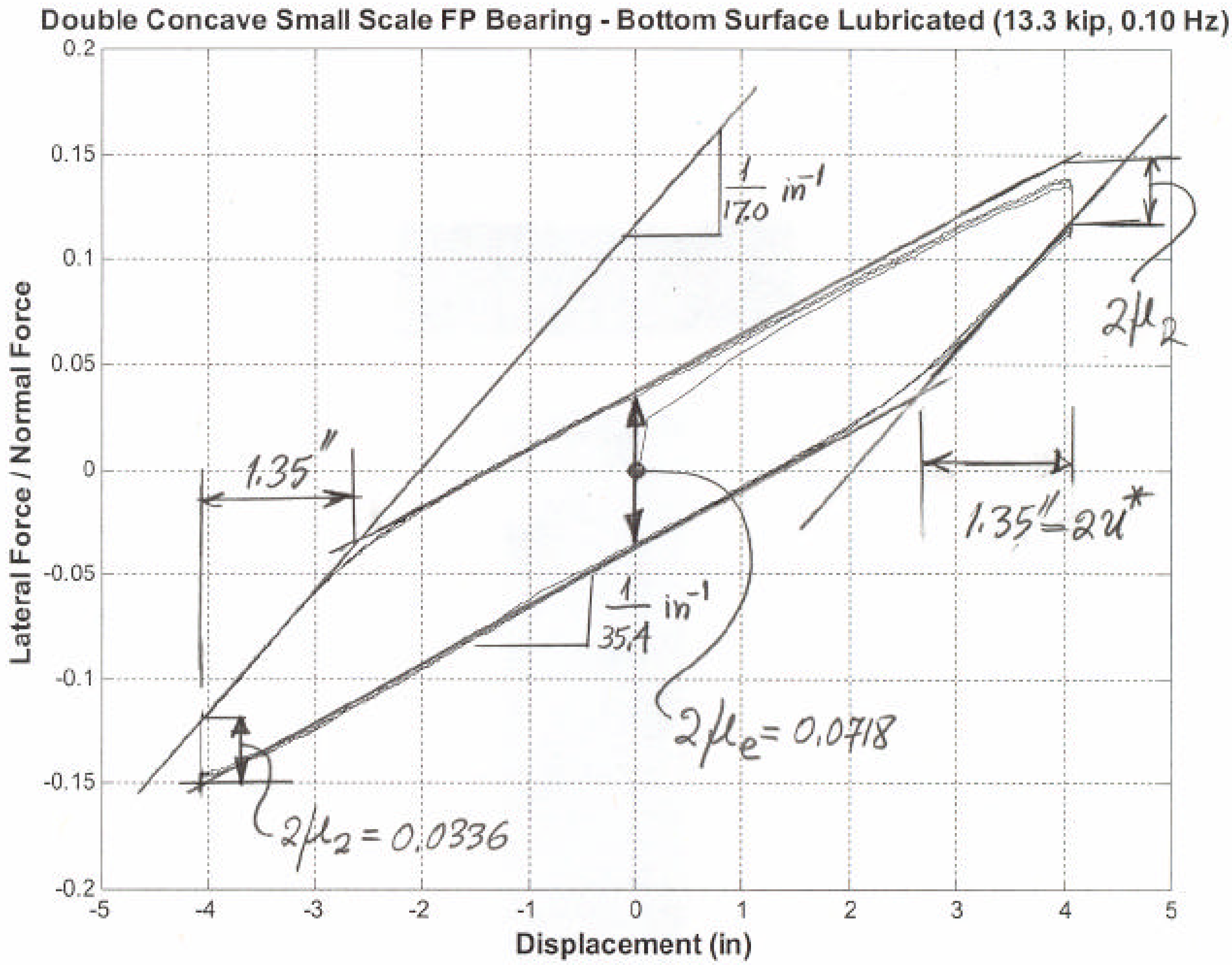

Figure 16: Graphical estimation of parameters from recorded loops of normalized lateral force-lateral displacement in test on small scale FP bearing with unequal coefficients of friction at the two sliding interfaces

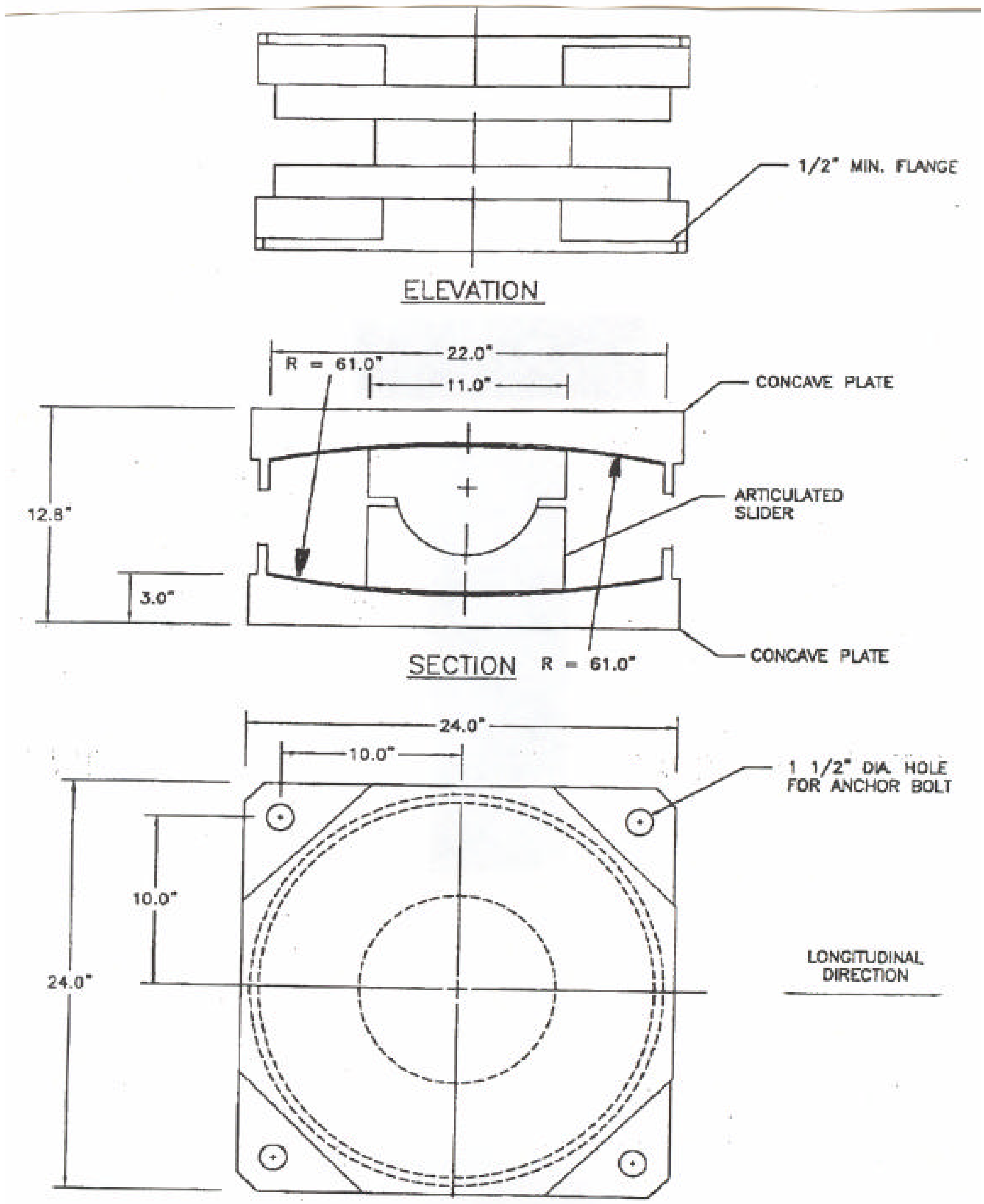

Figure 17: Demonstration FP-DC bearing tested by EPS, Inc.

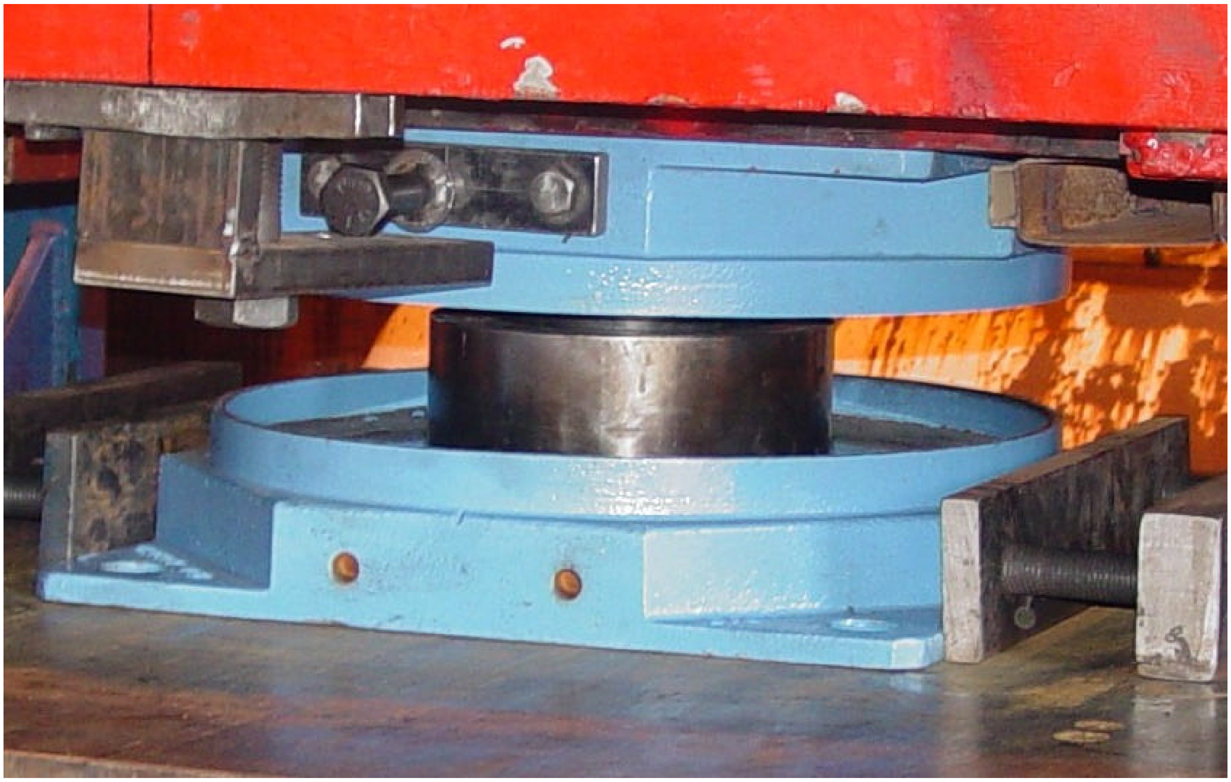

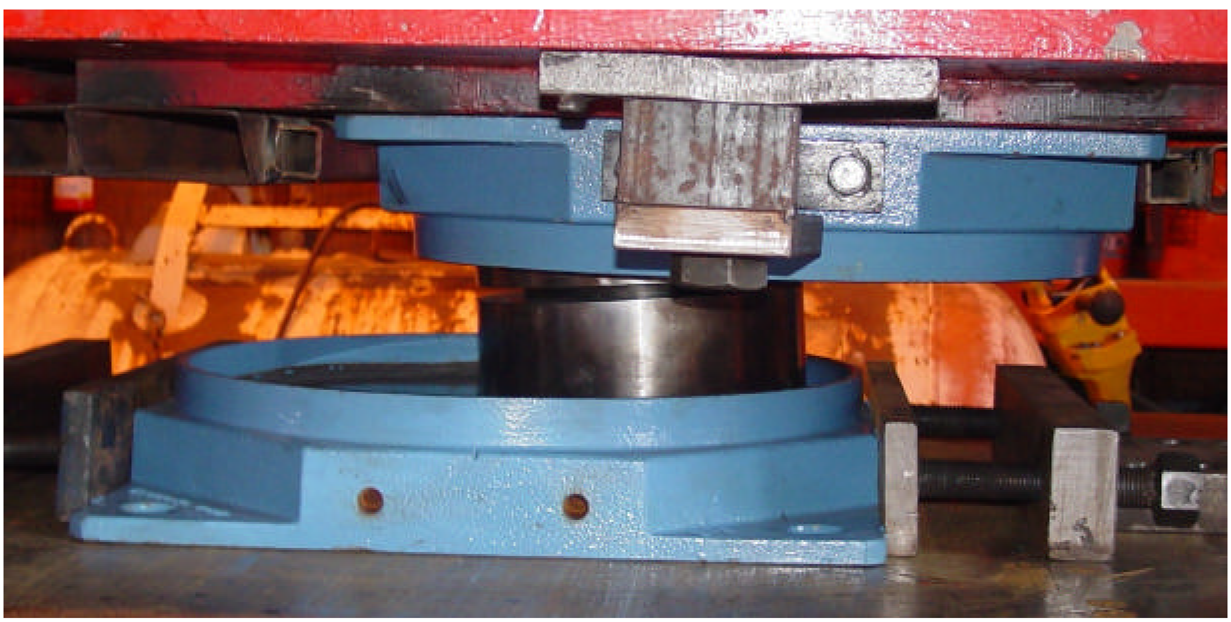

Figure 18: Views of demonstration FP-DC bearing tested by EPS, Inc.

APPENDIX A

EXPERIMENTAL RESULTS FOR DEMONSTRATION FP-DC BEARING

IDEAL R

$$\frac{1}{k} = \frac{1}{k_1} + \frac{1}{k_2}$$

$$\frac{R_{EFF}}{W} = \frac{R_1 - \frac{H_s}{2}}{W} + \frac{R_2 - \frac{H_s}{2}}{W}$$

$$\boxed{R_{EFF} = R_1 + R_2 - H_{SLIDER}}$$

$$= 61'' + 61'' - 8.5''$$

$$= 113.5''$$

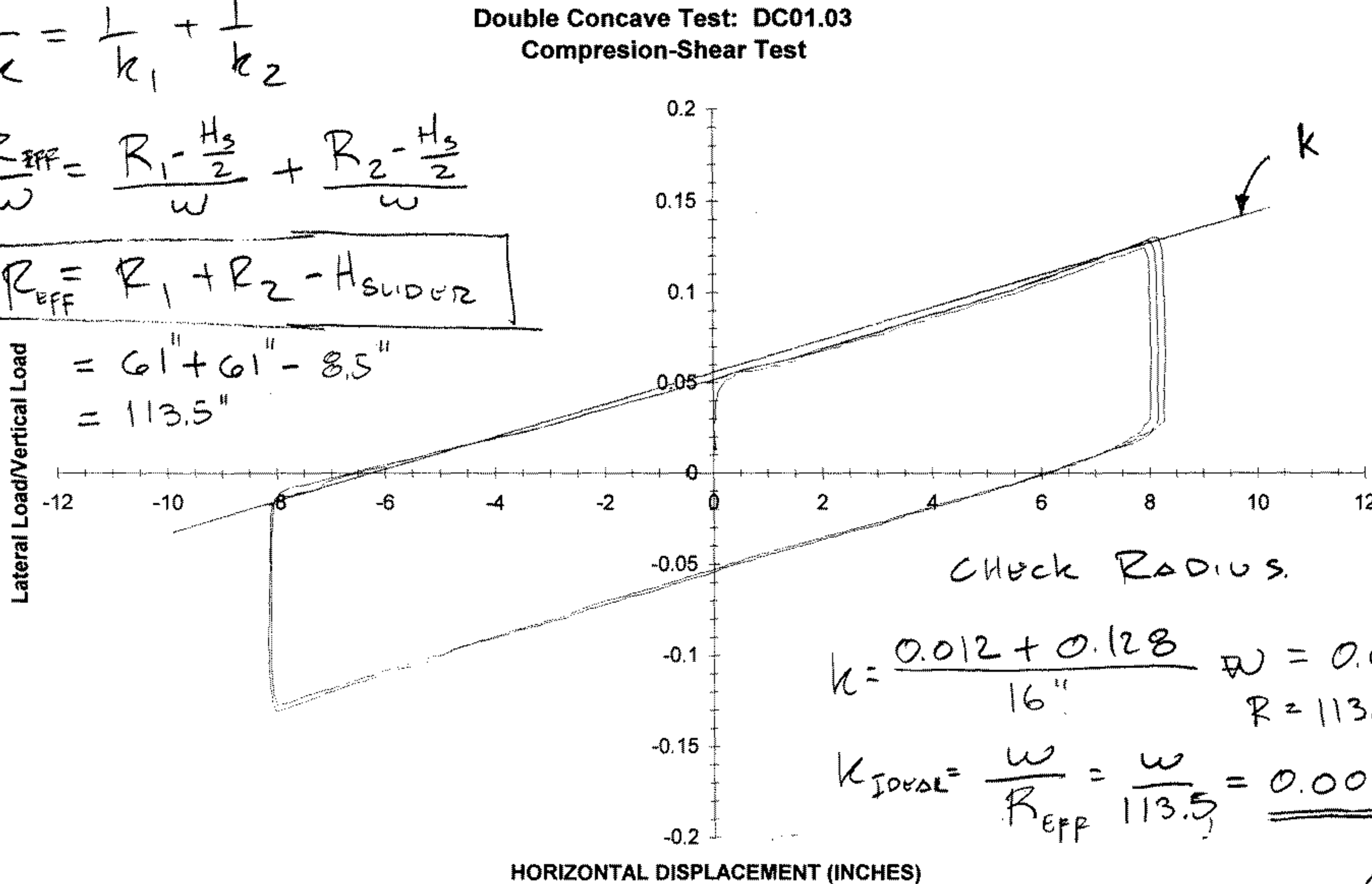

CHECK RADIUS

$$k = \frac{0.012 + 0.128}{16''} W = 0.0088W$$

$$R = 113.6''$$

$$k_{IDEAL} = \frac{W}{R_{EFF}} = \frac{W}{113.5} = \underline{\underline{0.0088\ W}}$$

<u>Ok</u>

Vertical Load (kips)
Avg. = 250

Double Concave Test: DC01.04
Compresion-Shear Test

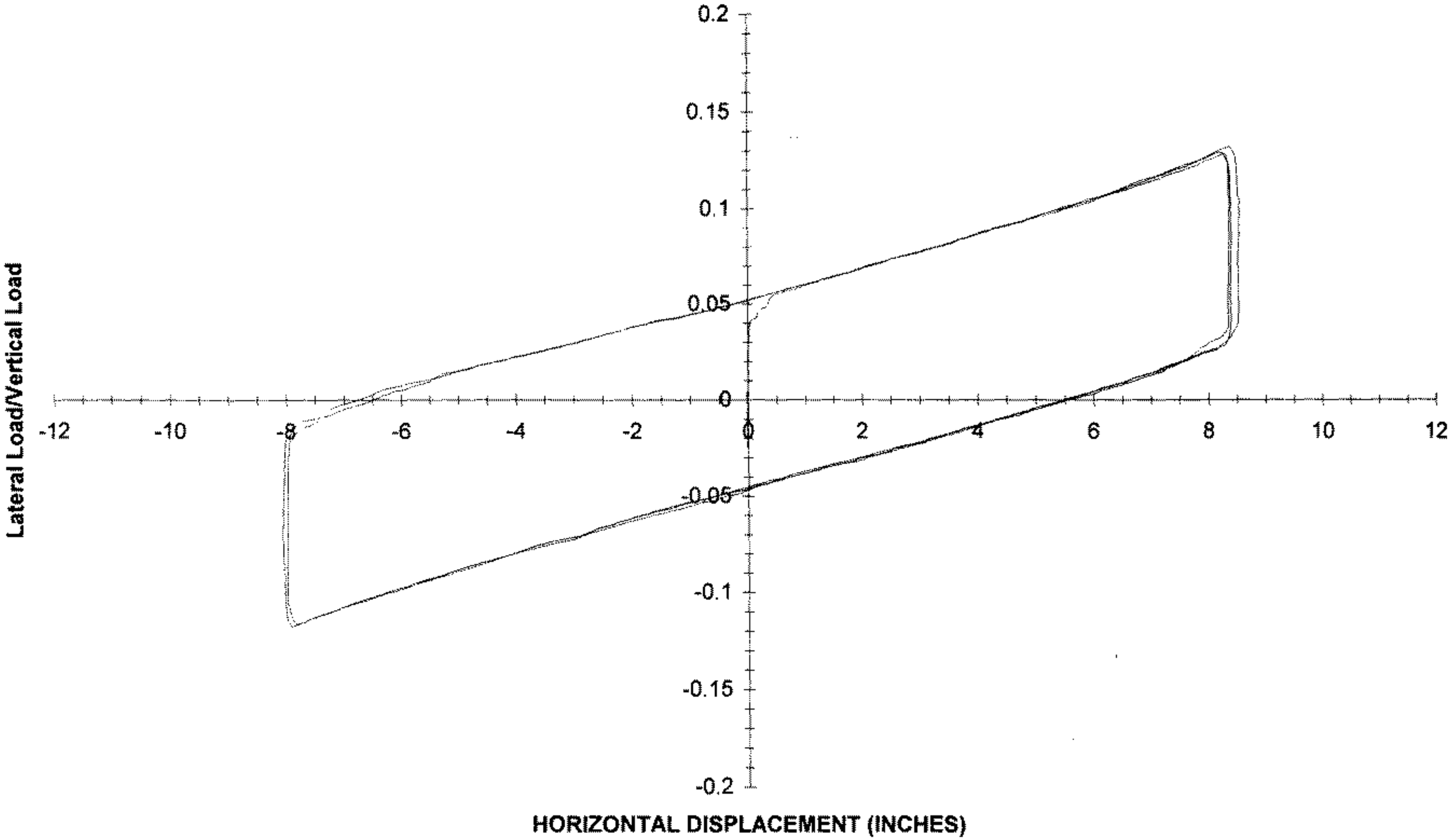

Vertical Load (kips)
Avg. = 391

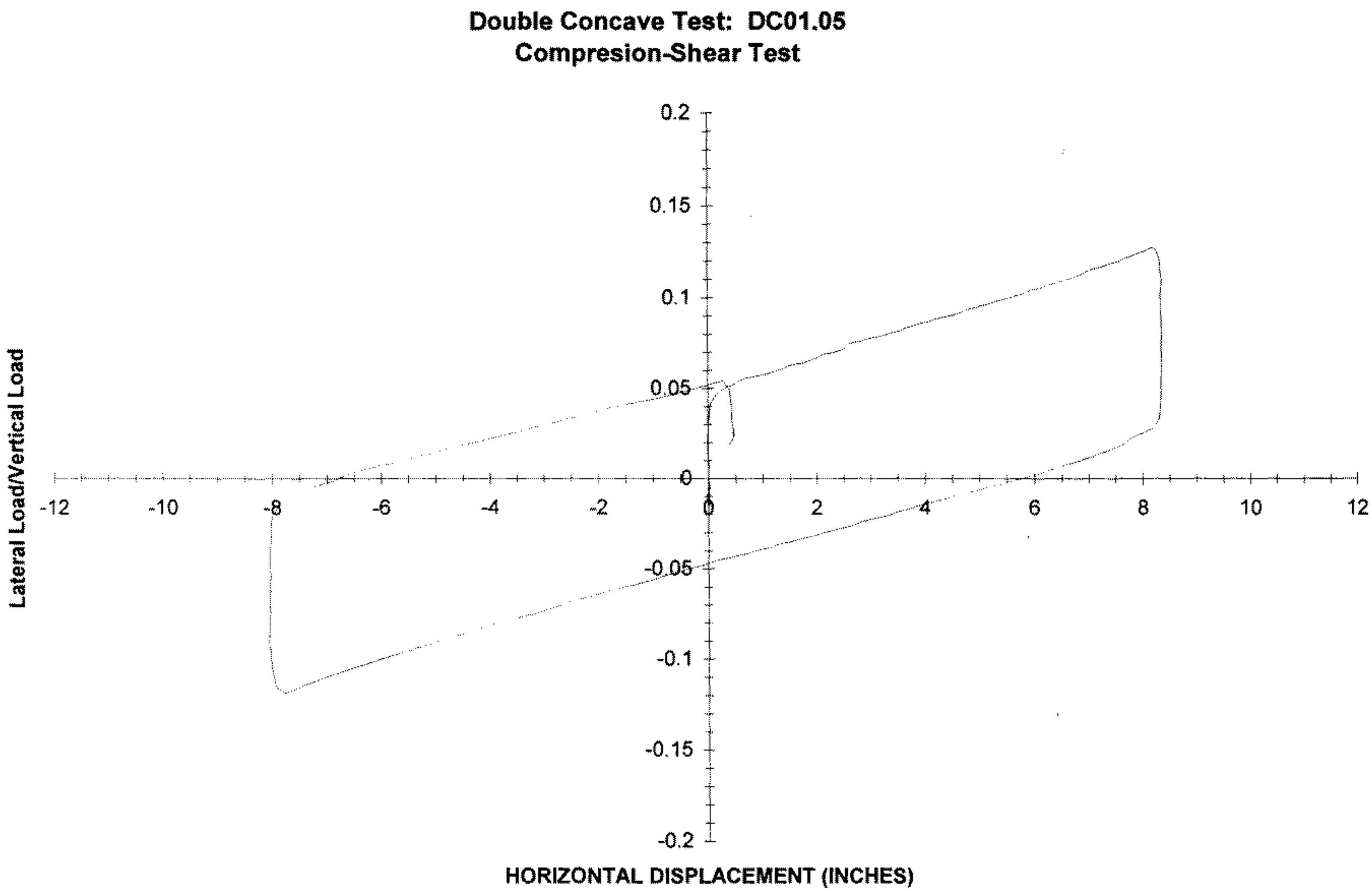

Vertical Load (kips)
Avg. = 424

Double Concave Test: DC01.06
Compresion-Shear Test

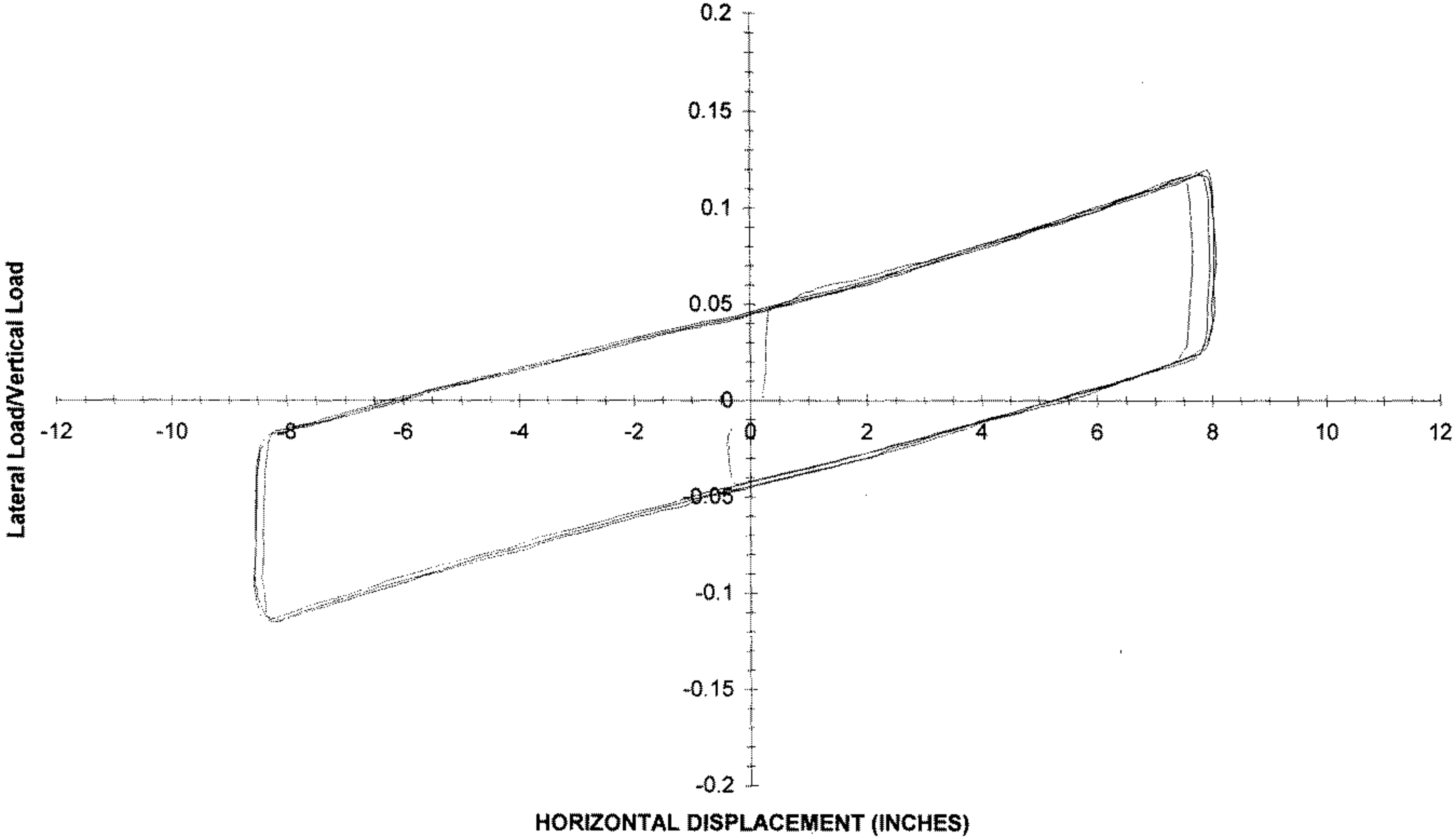

Vertical Load (kips)
Avg. = 603

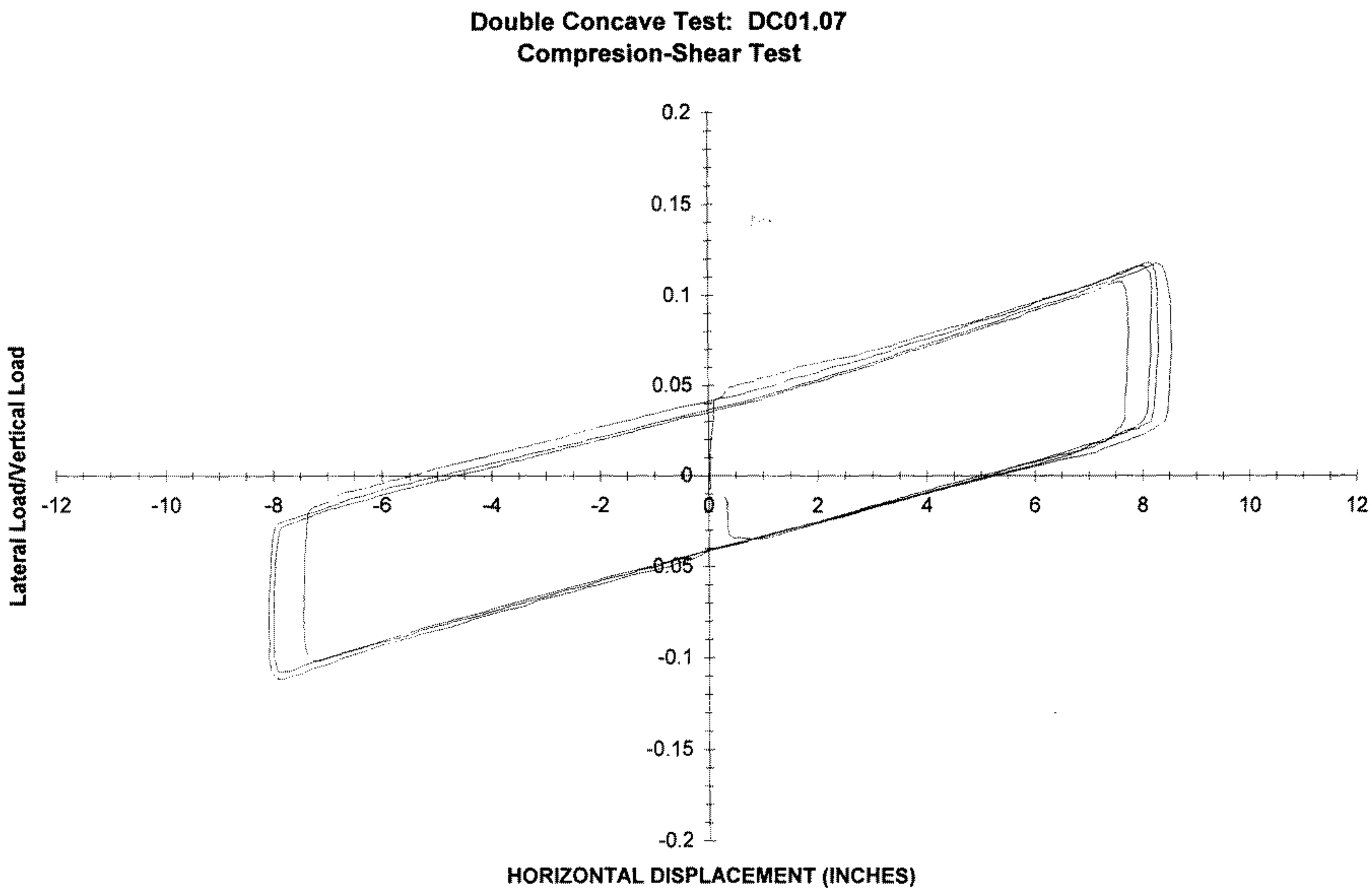

Vertical Load (kips)
Avg. = 891

Double Concave Test: DC01.08
Compresion-Shear Test

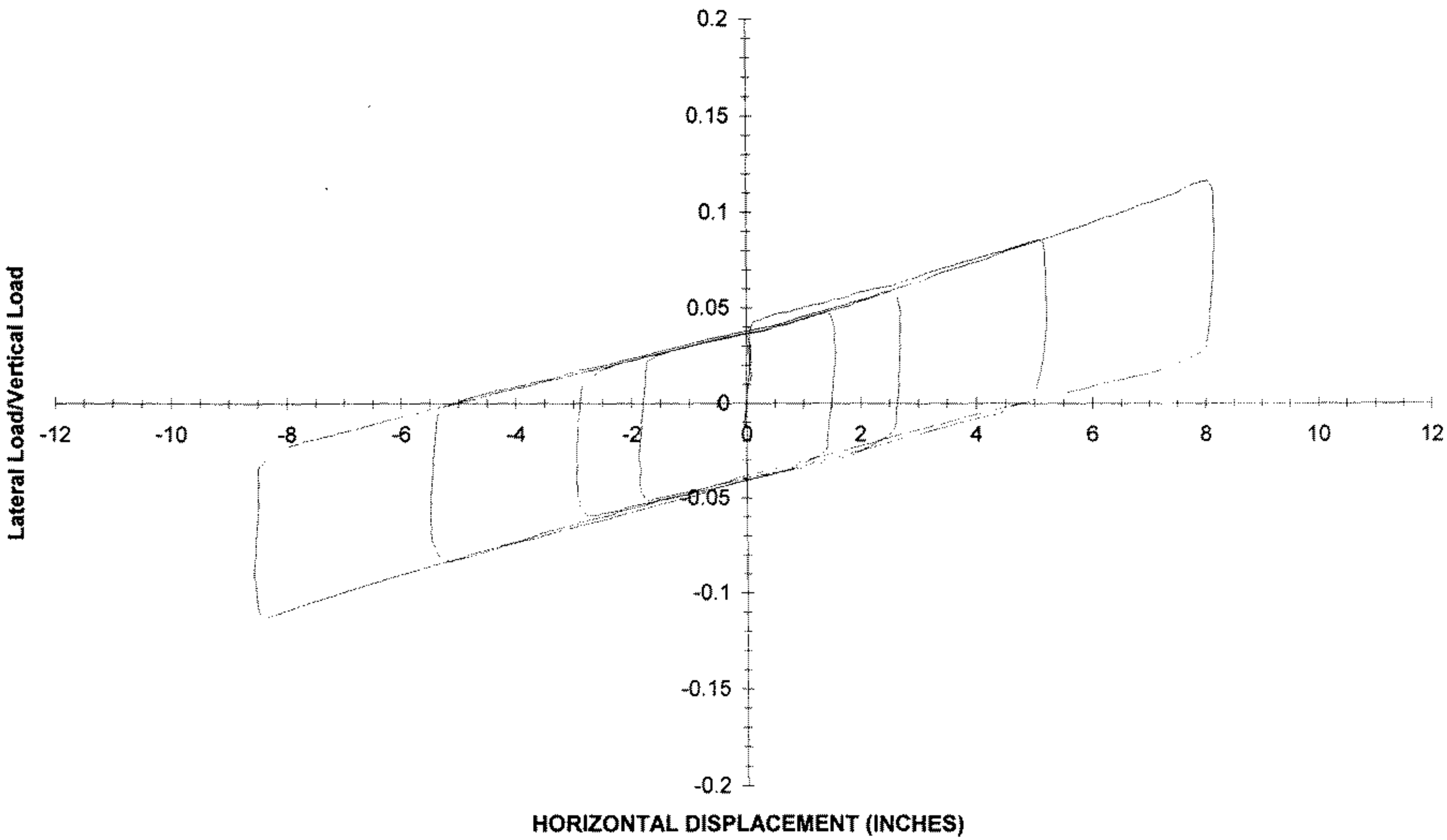

Vertical Load (kips)
Avg. = 940

Double Concave Test: DC01.09
Compresion-Shear Test

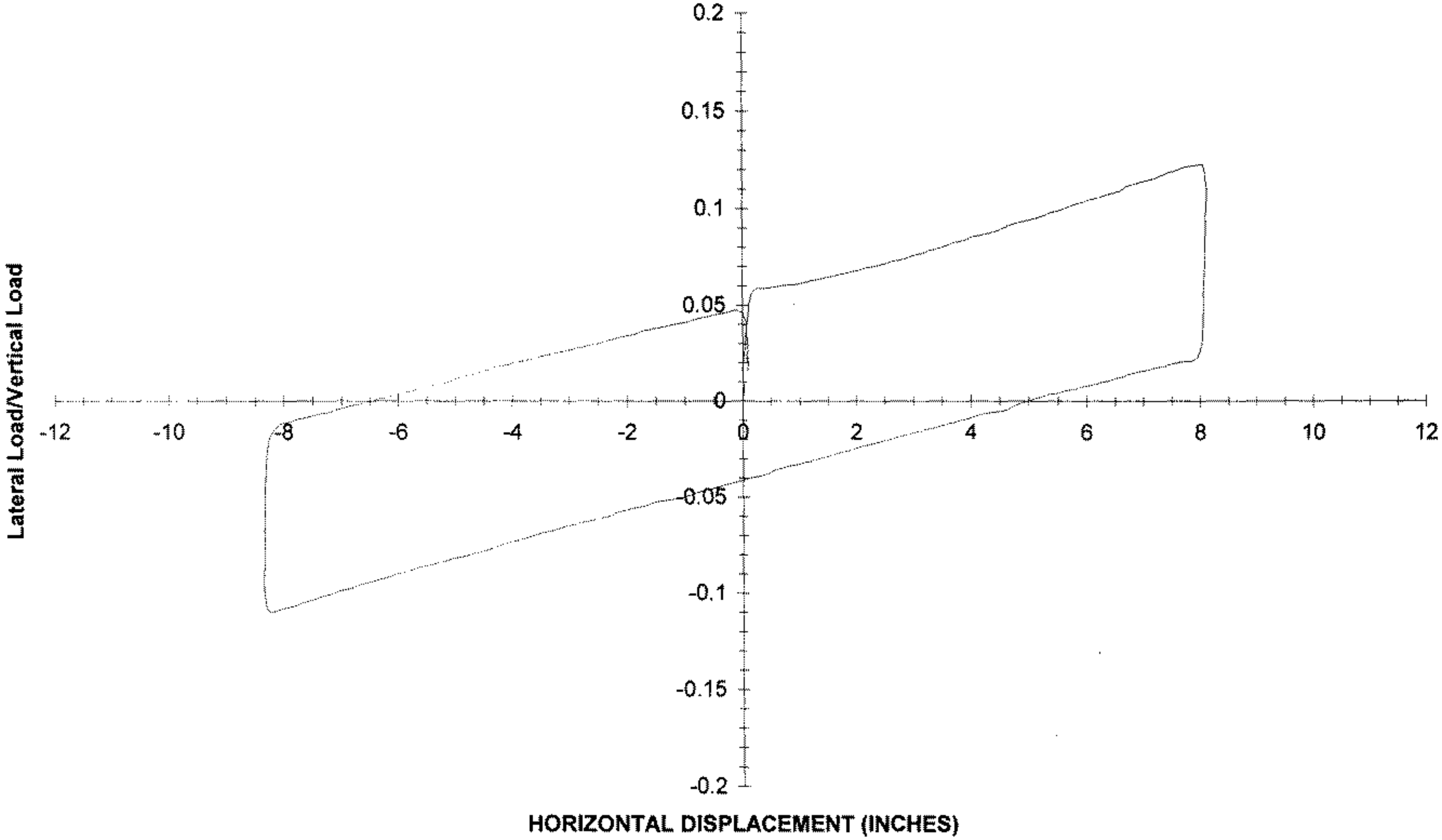

Vertical Load (kips)
Avg. = 892

Double Concave Test: DC01.10
Compresion-Shear Test

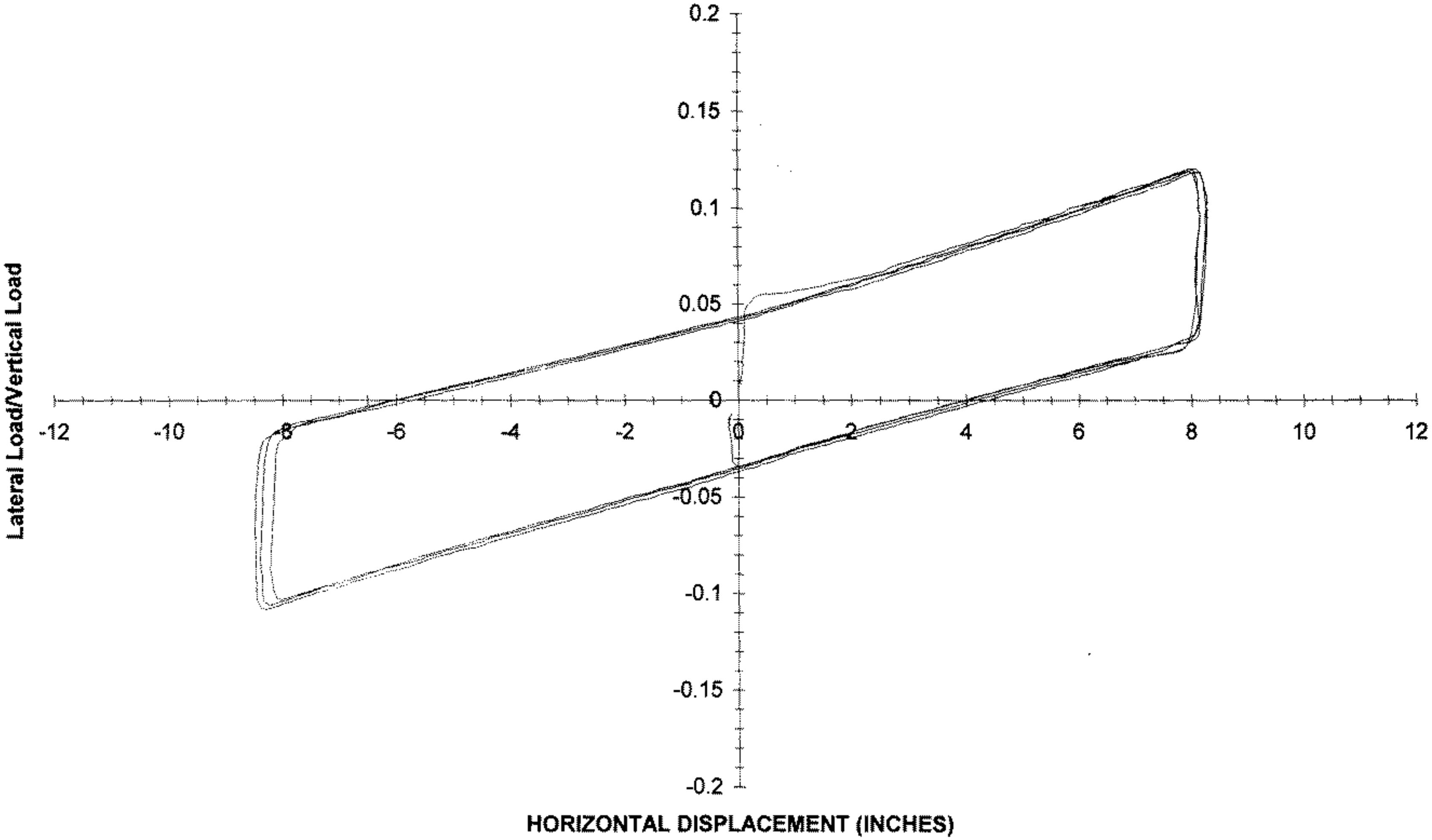

Vertical Load (kips)
Avg. = 1270

APPENDIX B

EXPERIMENTAL RESULTS FOR FP-DC BEARING FOR TESLIN RIVER BRIDGE, YUKON, CANADA

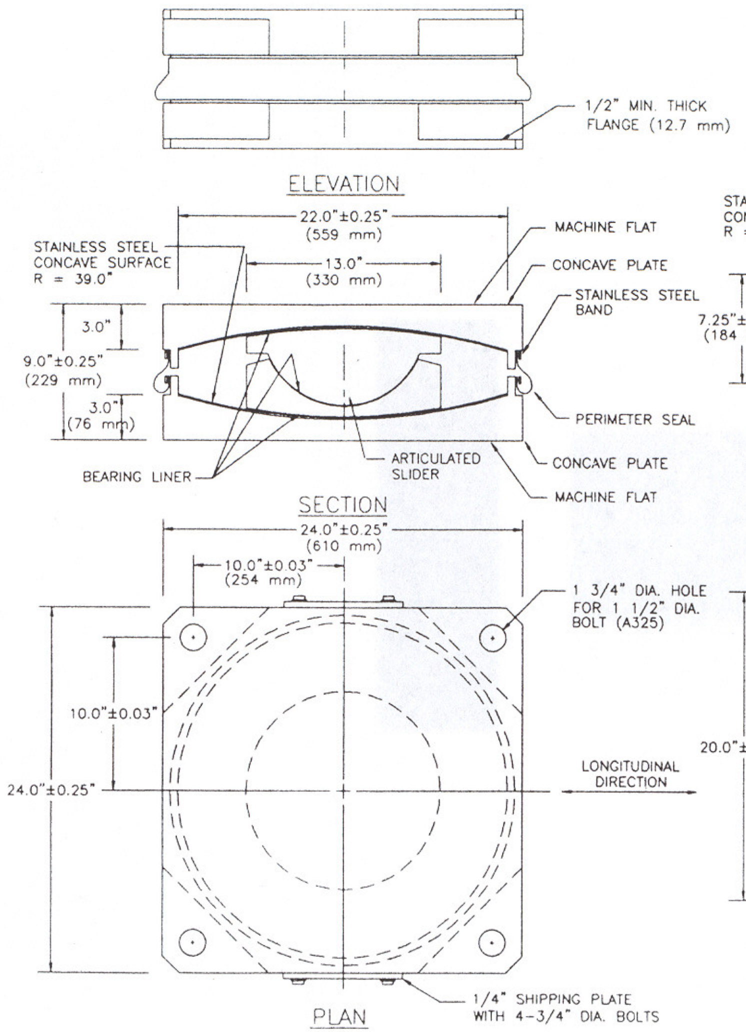

BEARING TYPE LARGE

FRICTION PENDULUM BEARING DFP3922-13
EFFECTIVE RADIUS = 2xR-H(SLIDER) = 74 IN. (1880 mm)
BEARING PERIOD = 2.75 SEC. (EFFECTIVE RADIUS = 74.0")
DISPLACEMENT CAPACITY = ±9.0" (228 mm)
ROTATION CAPACITY = ±2.0 DEG.
LOCATIONS: PIERS 2, 3, 4 & 5
QUANTITY = 8

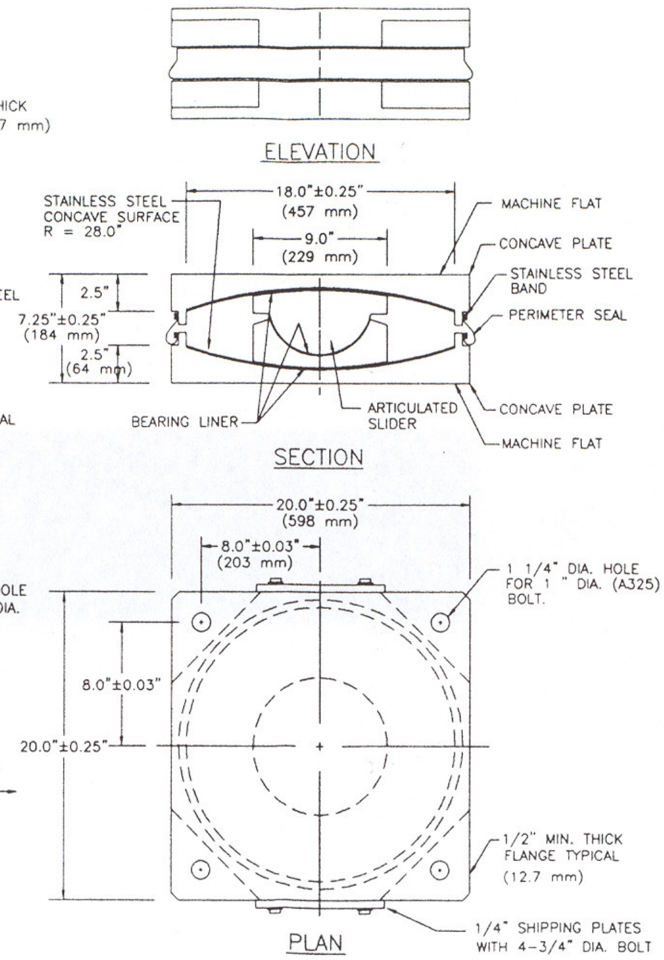

BEARING TYPE SMALL

FRICTION PENDULUM BEARING DFP2818-9
EFFECTIVE RADIUS = 2xR-H(SLIDER) = 50 IN. (1270 mm)
BEARING PERIOD = 2.25 SEC. (EFFECTIVE RADIUS = 50.0")
DISPLACEMENT CAPACITY = ±9.0" (228 mm)
ROTATION CAPACITY = ±2.0 DEG.
LOCATIONS: ABUT NO. 1 & 2 PIERS 0, 1, 1A, 2, 5, 6 & 7
QUANTITY = 28

GENERAL NOTES:

1. BEARING PROPERTIES

   BEARING TYPE LARGE: DYNAMIC PERIOD (T) = 2.75 SECONDS
   EFFECTIVE RADIUS =74 INCHES (1880 mm)
   DYNAMIC FRICTION = 7%

   BEARING TYPE SMALL: DYNAMIC PERIOD (T) = 2.50 SECONDS
   EFFECTIVE RADIUS = 50.0 INCHES (1270 mm)
   DYNAMIC FRICTION = 10%

2. MATERIAL SPECIFICATIONS
   THE MATERIAL OF THE MAIN CONCAVE SPHERICAL SURFACE SHALL BE ASTM DESIGNATION A240, TYPE 316 STAINLESS STEEL. THE MATERIAL OF THE CONCAVE PLATE SHALL BE A536 GRADE 65-45-12 WITH A MIN. YIELD STRENGTH OF 40 KSI., MIN. ULTIMATE TENSILE STRENGTH OF 60 KSI. AND MIN. ELONGATION OF 12%. THE MATERIAL OF THE ARTICULAING SLIDER SHALL BE TYPE 304 STAINLESS STEEL. THE SEAL MATERIAL SHALL BE AN ETHYLENE PROPYLENE MATERIAL. MISC. STEEL MATERIAL SHALL BE ASTM A36.

3. PAINT SPECIFICATIONS
   ALL METAL SURFACES ON THE BEARING (EXCLUDING STAINLESS STEEL) EXPOSED TO THE ATMOSPHERE, SHALL BE BLASTED TO SSPC/SP-10, PAINTED WITH ONE COAT, 2.5 MILS DFT, OF INORGANIC ZINC PRIMER, ONE INTERMEDIATE COAT, 3.5 MILS MIN. DFT, OF EPOXY, AND ONE FINISH COAT, 2.0 MIL, DFT, OF URETHANE. FINISH COAT COLOR TO BE PROVIDED BY THE CONTRACTOR. BOTTOM & TOP SURFACE OF BEARING SHALL BE PRIMER PAINTED ONLY.

4. TOLERANCES
   THE EXTERNAL BEARING DIMENSIONS SHALL BE WITHIN ±25 IN. OF THE VALUES SHOWN IN THESE DRAWING. THE INTERNAL BEARING DIMENSIONS SHALL BE PER EPS STANDARD MANUFACTURING PROCESS. THE LOCATION OF HOLES OR THREADED HOLES WILL BE LOCATED TO WITHIN ±0.03 IN. OF THE VALUES SHOWN IN THE DRAWINGS. THICKNESS OF LINER MATERIAL FOR SLIDER IS 0.04 IN. MIN. THICKNESS OF LINER MATERIAL FOR HOUSING CUP IS 0.02 IN. MIN. THICKNESS OF STAINLESS STEEL OVERLAY MATERIAL FOR CONCAVE PLATE IS 0.10 IN. MIN. SURFACE MACHINE FLAT SHALL HAVE A MILLED SURFACE FINISH WITH ROUGHNESS VALUE NOT EXCEEDING 500. THE FLATNESS TOL: MAX. GAP UNDER A PRECISION STRAIGHT-EDGE SHALL BE LESS THAN 1/8" ACROSS THE SURFACE.

5. INSTALLATION NOTES
   A. MOUNTING PLATE HOLES AND ANCHOR BOLTS TO BE SET BY TEMPLATE. DO NOT SET MOUNTING PLATE HOLES OR ANCHOR BOLTS BASED ON PLAN DIMENSIONS.
   B. LEVEL THE CONCAVE PLATE AT THE MID-POINT OF THE FOUR SIDE TO BE LEVEL TO WITHIN 1/16 INCH (1.6 mm) PER FOOT.
   C. NO BEARING COMPONENTS SHALL BE HEATED ABOVE 250°F. (121°C) IF HEATING ABOVE THIS TEMPERATURE IS REQUIRED, THE HEATING PROCEDURE SHOULD BE REVIEWED BY EPS ENGINEER.
   D. BEARINGS ARE SHIPPED WITH TEMPORARY SHIPPING PLATES. THESE PLATES SHALL BE REMOVED AFTER INSTALLATION AND AS DIRECTED BY THE PROJECT ENGINEER.
   F. MAXIMUM VERTICAL LOAD ON BEARINGS PRIOR TO GROUTING OR INSTALLATION OF BEARING PAD IS 1,000 POUNDS (4.46 kn). BEARINGS SHALL NOT BE STACKED MORE THAN TWO BEARINGS TALL.

TESLIN RIVER BRIDGE REHABILITATION ALASKA HIGHWAY #1, km1296 OWNER: YUKON INFRASTRURE, CANADA CONTRACTOR: KETZA CONSTRUCTION CORPORATION 107 PLATINUM ROAD, WHITEHORSE, YUKON				EARTHQUAKE PROTECTION SYSTEMS 451 AZUAR DRIVE, BLDG. 759, MARE ISLAND VALLEJO, CA. 94592 TEL: (707) 644-5993 FAX: (707) 644-5995		
FRICTION PENDULUM BEARING DETAILS AND GENERAL NOTES	REVISIONS	DATE	BY	DRAWN BY: SL CHECKED BY: VZ	DATE	DRAWING FP-1

BEARING TESTING PROCEDURE

A. THE EFFECTIVE RADIUS AND DYNAMIC FRICTION FOR THE PROPERTY COMBINED COMPRESSION AND SHEAR TEST IS LISTED IN THE BEARING PROPERTY TABLE BELOW.

B. ONE TYPE LARGE AND ONE TYPE SMALL BEARING WILL BE TESTED PER SECTION 01400-3.19 "PENDULUM BEARING TESTING" OF THE PROJECT SPECIFICATIONS WITH THE LOAD AND DISPLACEMENTS LISTED BELOW.

C. TESTING TOLERANCE: THE AVERAGE VERTICAL LOAD SHALL BE WITH ±10% OF THE TARGET LOAD. THE AVERAGE DISPLACEMENT SHALL BE WITHIN ±10% OF THE TARGET DISPLACEMENT.

D. THE DYNAMIC FRICTION IS THE AVERAGE OF THE THREE CYCLE TEST. THE FRICTION PER CYCLE IS CALCULATED BY DIVIDING THE EDC WITH THE AVERAGE VERTICAL LOAD (EDC/P(AVG.). EDC IS THE ENERGY DISSIPATED PER CYCLE (AREA OF THE HYSTERSIS LOOP).

BEARING PROPERTY TABLE

	BEARING TYPE	
	LARGE	SMALL
Design Displacement D (inches)	8.0	8.0
Average Vertical Dead Load (kips)	475	136
Effective Radius (in.)	74	50
Dynamic Friction	0.07	0.10

DYNAMIC FRICTION TOLERANCE

TEMPERATURE	LARGE BEARING		SMALL BEARING	
+104°F	0.07	+0.00 −0.03	0.10	+0.00 −0.04
+30°F	0.07	+0.01 −0.01	0.10	+0.01 −0.01
−51°F	0.07	+0.03 −0.00	0.10	+0.04 −0.00

BEARING TESTING LOADS AND DISPLACEMENT TABLE

Testing Designation	Specification Section	Number of Cycles	Bearing Type Large		Bearing Type Small		Bearing Temperature (Deg. F)
			Vertical Load (kips)	Lateral Displacement (inches)	Vertical Load (kips)	Lateral Displacement (inches)	
Temperature Property Test	01400 3.19.3	3 3 3 3 3	136	±8.0 ±8.0 ±8.0 ±8.0 ±8.0	475	±8.0 ±8.0 ±8.0 ±8.0 ±8.0	70±9 −51±9 30±9 104±9 70±9
Static Property Test	01400 3.19.4	1 20	136	±0.8 ±1.6	475	±0.8 ±1.6	70±15 70±15
Dynamic Property Test	01400 3.19.5	3 3 3 20	136	±2.0 ±4.0 ±6.0 ±8.0	475	±2.0 ±4.0 ±6.0 ±8.0	70±15 70±15 70±15 70±15
Pressure Property Test	01400 3.19.6	3 3 3 3 3	64 191 316 445 572	±4.0 ±4.0 ±4.0 ±4.0 ±4.0	531 796 1061 1194	±4.0 ±4.0 ±4.0 ±4.0	70±15 70±15 70±15 70±15 70±15

TESLIN RIVER BRIDGE REHABILITATION ALASKA HIGHWAY #1, km1296 OWNER: YUKON INFRASTRURE, CANADA CONTRACTOR: KETZA CONSTRUCTION CORPORATION 107 PLATINUM ROAD, WHITEHORSE, YUKON			EARTHQUAKE PROTECTION SYSTEMS 451 AZUAR DRIVE, BLDG. 759, MARE ISLAND VALLEJO, CA. 94592 TEL: (707) 644-5993 FAX: (707) 644-5995		
TESTING PROCEDURE	REVISIONS	DATE	BY	DRAWING BY: SL CHECKED BY: VZ	DATE	DRAWING FP-2

Teslin River Bridge Bearing Test - Prototype Bearing B-1
Pressure Property Test

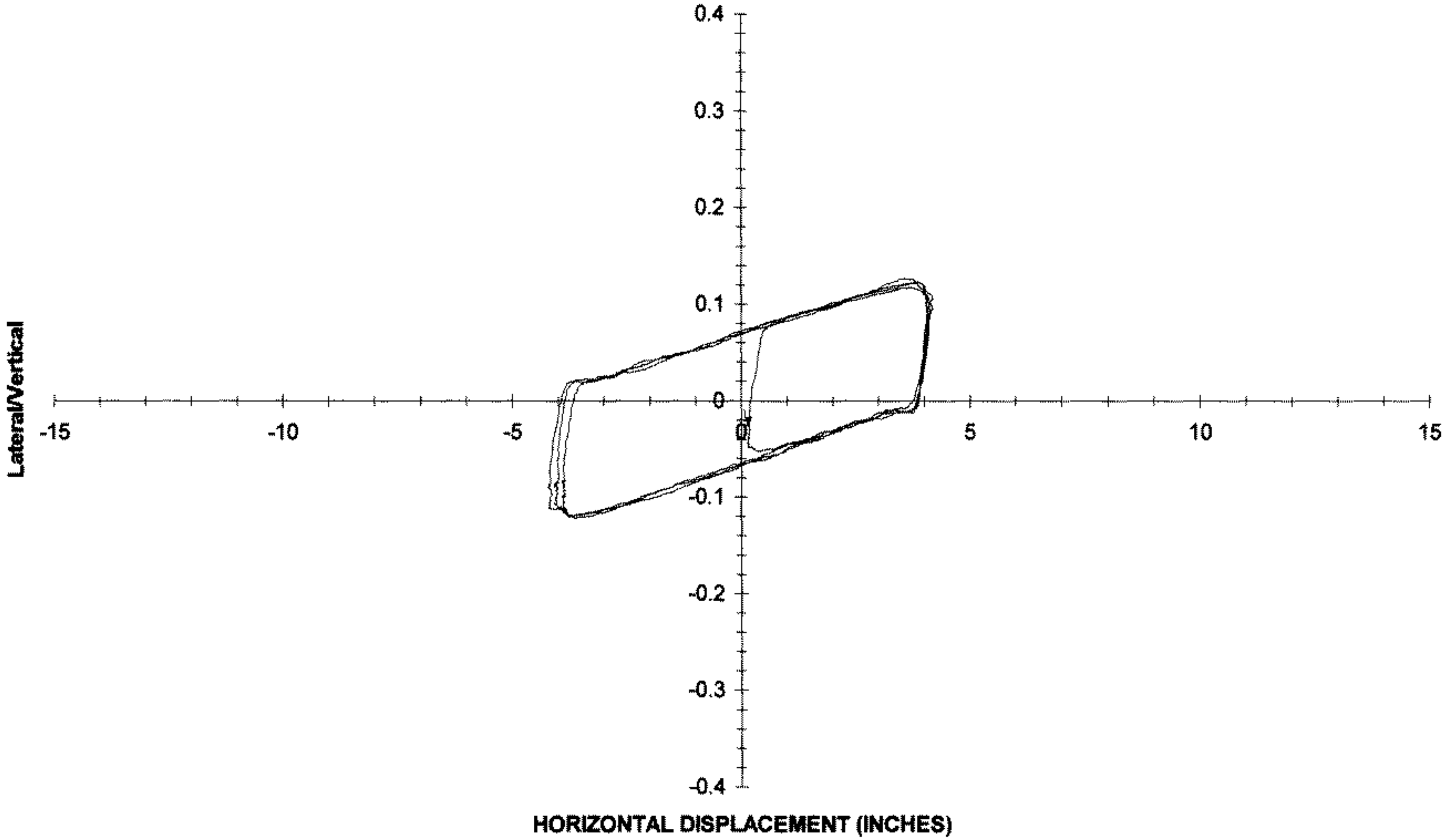

Vertical Load (kip)
Avg. = 806

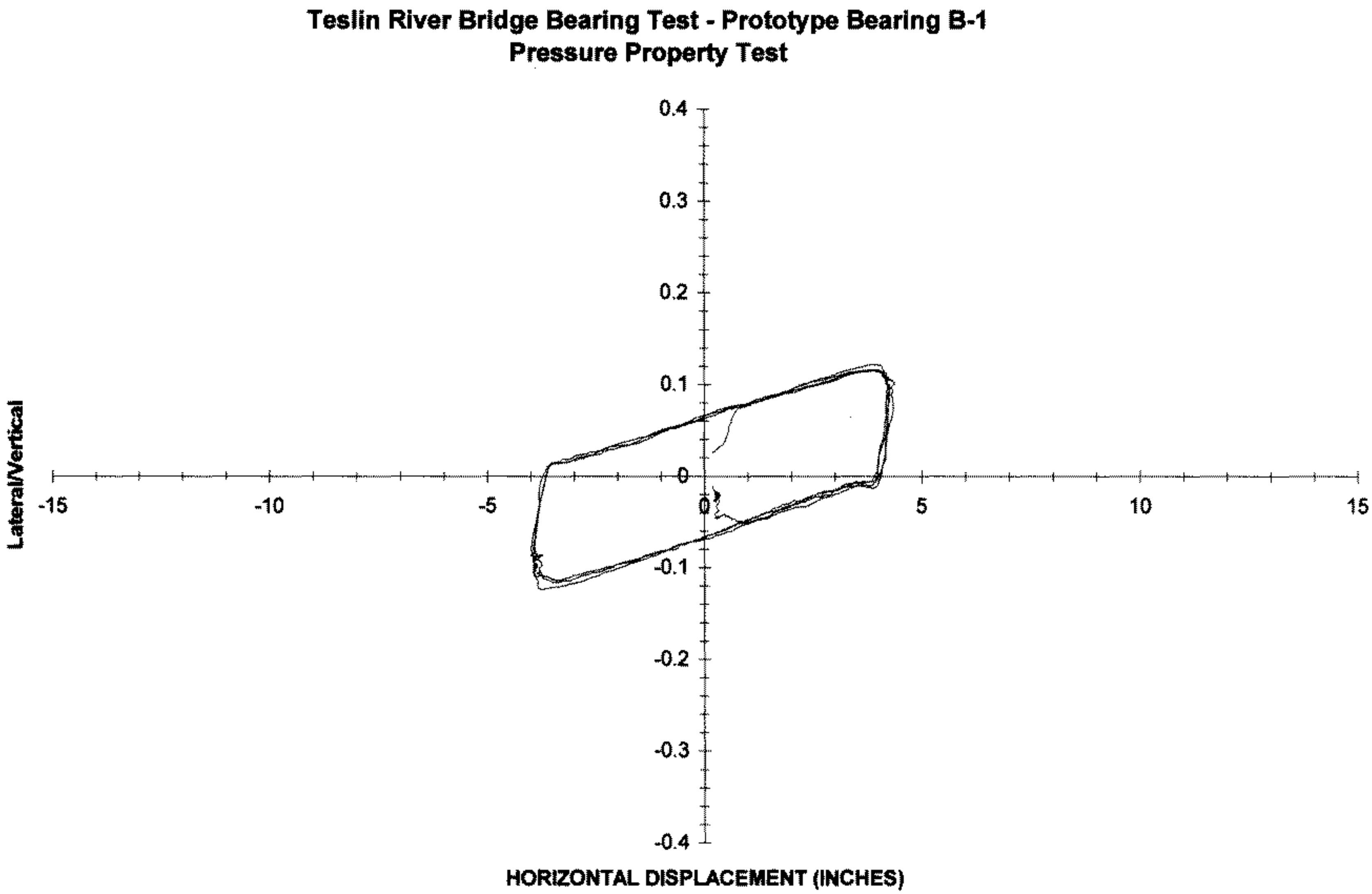

Vertical Load (kip)
Avg. = 1015

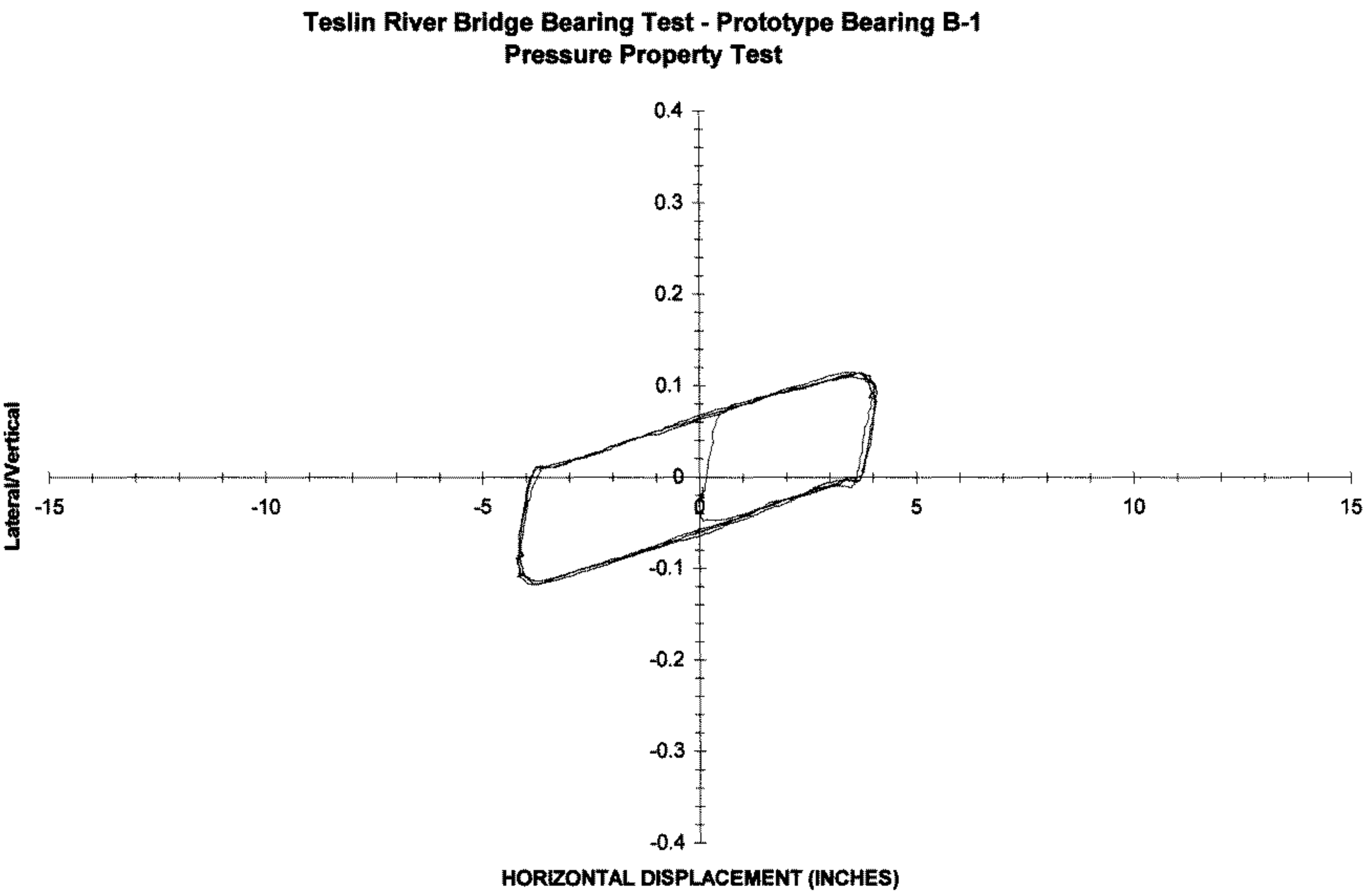

Vertical Load (kip)
Avg. = 1183